DOI: 10.1002/cmdc.201000065

The Role of Fluorine Substitution in Biphenyl Methylene Imidazole-Type CYP17 Inhibitors for the Treatment of Prostate Carcinoma

Qingzhong Hu,[a] Matthias Negri,[a] Sureyya Olgen,[a, b] and Rolf W. Hartmann*[a]

It has been established that the growth of most prostate carcinomas depends on androgen stimulation. The inhibition of cytochrome P450-17 (CYP17) to block androgen biosynthesis is therefore regarded as a promising approach to therapy. Based on our previously identified lead compound **Ref 1**, a series of fluorine-substituted biphenyl methylene imidazoles were designed, synthesized, and evaluated as CYP17 inhibitors to elucidate the influence of fluorine on in vitro and in vivo activity. It was found that *meta*-fluoro substitution at the C ring improved activity, whereas *ortho* substitution decreased potency. Docking studies performed with our human CYP17 homology model suggest the presence of multipolar interactions between fluorine and Arg109, Lys231, His235, and Glu305. As expected, introduction of fluorine also prolonged the half-life in plasma. The SARs obtained confirm the reliability of the protein model; compound **9** ($IC_{50} = 131$ nM) was identified as a strong CYP17 inhibitor, showing potent activity in rat, high bioavailability, and a long plasma half-life: 12.8 h.

Introduction

As the most common malignancy in elder men, prostate carcinoma is a major cause of death.[1] It has been established that the growth of up to 80% of prostate carcinomas depends on androgen stimulation. Therefore, the segregation of tumor cells from androgen hormones would effectively prevent cancer cell proliferation. Because >90% of testosterone is produced in the testes, orchidectomy or treatment with gonadotropin-releasing hormone (GnRH) analogues[2] (chemical castration) are applied in the clinic. As this therapy has no effect on the minor amounts of androgen produced in the adrenal glands, androgen receptor antagonists are used in conjunction. This is the current standard therapy for prostate carcinoma, the so-called "combined androgen blockade" (CAB).[3] However, CAB often leads to resistance, which can be associated with androgen receptor mutations. The mutated androgen receptor recognizes antagonists and glucocorticoids as agonists, ultimately resulting in the collapse of CAB therapy.[4]

The shortcomings of CAB warrant a more promising alternative: total blockage of androgen biosynthesis, which means the inhibition of cytochrome P450-17 (17α-hydroxylase-17, 20-lyase, CYP17). CYP17 is one of six CYP enzymes involved in steroid biosynthesis. Like all CYP enzymes, CYP17 consists of a heme and an apoprotein moiety. Although all potent inhibitors interfere with the heme (which is common to all CYP enzymes) by complexing its central iron ion, it is nevertheless possible to selectively inhibit these enzymes, as has been demonstrated with CYP19 (aromatase, estrogen synthase)[5] and CYP11B2 (aldosterone synthase).[6] Whereas CYP19 inhibitors are already in clinical use,[5a] the first highly potent and selective CYP11B2 inhibitors were just recently identified,[6] some of which are extremely selective.

CYP17, located in both testicular and adrenal tissues,[7] is the key enzyme that catalyzes the conversion of pregnenolone and progesterone to dehydroepiandrosterone (DHEA) and androstenedione, respectively. DHEA can be transformed into androstenedione by 3β-hydroxysteroid dehydrogenase (3β-HSD), followed by its subsequent conversion into the most potent androgen, dihydrotestosterone (DHT), in androgen target cells through two enzymatic steps catalyzed by 17β-HSD1 or 17β-HSD3 and steroid 5α-reductase (5αR). Thus, inhibition of CYP17 could block androgen production in testes as well as adrenal tissue. Furthermore, targeting genetically stable healthy tissue instead of cancer cells would circumvent resistance caused by mutation.

Ketoconazole (Figure 1), an antimycotic agent that shows nonselective inhibition of CYP17, is the first medication which has been used clinically in the treatment of prostate carcinoma. Although withdrawn because of side effects, ketoconazole shows good curative properties,[8] which demonstrates the feasibility of prostate carcinoma treatment via CYP17 inhibition. Since then, in mimicry of the physiological substrates, many steroidal CYP17 inhibitors were synthesized by others[9] as well as our research group;[10] among these, abiraterone (Figure 1) recently entered phase II clinical trials. However, the affinity of

[a] *Q. Hu,[+] M. Negri,[+] Dr. S. Olgen, Prof. Dr. R. W. Hartmann*
Pharmaceutical and Medicinal Chemistry, Saarland University
P.O. Box 151150 & Helmholtz Institute for Pharmaceutical Research
Saarland (HIPS), 66041 Saarbrücken (Germany)
Fax: (+49) 681-302-70308
E-mail: rwh@mx.uni-saarland.de
Homepage: http://www.PharmMedChem.de

[b] *Dr. S. Olgen*
Present address: *University of Ankara, Faculty of Pharmacy*
Tandogan, Ankara 06100 (Turkey)

[+] These authors contributed equally to this work.

Supporting information for this article is available on the WWW under http://dx.doi.org/10.1002/cmdc.201000065.

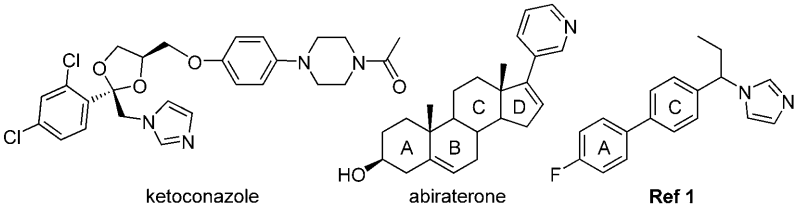

Figure 1. Typical CYP17 inhibitors.

steroidal compounds toward steroid receptors, which often results in side effects regardless of whether the compound in question acts as an agonist or antagonist, prompted us to develop nonsteroidal CYP17 inhibitors.[11,12]

Our research group has reported a series of biphenyl methylene imidazoles as potent CYP17 inhibitors.[12] A promising lead compound 1-[1-(4′-fluorobiphenyl-4-yl)propyl]-1*H*-imidazole[12g] (**Ref 1**, Figure 1) was identified in the optimization process. In the present study this compound was further modified to increase its potency, selectivity, and to improve its pharmacokinetic properties. Fluorine is known to be able to form multipolar interactions with several amino acids,[13e–l] and it can also enhance metabolic stability; for these reasons, the biphenyl core was substituted with additional fluorine atoms, leading to compounds **1**–**22**. Exchanging the 1-imidazolyl group with a 5-imidazolyl moiety while maintaining 4-fluorophenyl as the A ring, compounds **23**–**26** were subsequently obtained. Furthermore, besides determination of inhibitory activities toward human CYP17 in vitro, selected compounds were examined for their ability to decrease plasma testosterone concentrations and for their pharmacokinetic properties in rats. Moreover, computational investigations were performed: molecular docking studies using our homology model of human CYP17[12e] to elucidate the enzyme–inhibitor interactions and quantum mechanical studies to explore the influence of fluorine substitution on the potency and pharmacokinetic properties of this type of CYP17 inhibitor.

Drug Design

Fluorine, as the most electronegative atom, forms strong C–F bonds and has therefore been widely used to prevent undesired metabolism. In addition to increased metabolic stability, fluorine can also improve other pharmacokinetic properties by influencing pK_a, elevating lipophilicity, and decreasing plasma protein binding.[13] Recently, multipolar interactions between fluorine and some amino acid residues responsible for enhanced binding potency have also been reported.[13e–l] Based on these findings, the concepts of fluorophilicity and fluorophobicity in protein active sites have been discussed,[13c,d] and systematic fluorine scans have been recommended for drug discovery and lead optimization efforts.

We found that fluorine substitution at the *para* position of the A ring could significantly increase the inhibitory potency of biphenyl methylene imidazole-type CYP17 inhibitors, resulting in compound **Ref 1** (IC_{50} = 345 nM).[12g] In addition to complex formation between a heterocyclic nitrogen atom of **Ref 1** and the heme iron center, recognized as the main anchor point for nonsteroidal CYP inhibitors (first noted for CYP19 inhibitors[5b–c]), polar interactions between the **Ref 1** fluorine atom and the guanidinium side chain of Arg109 and the amine group of Lys231 were observed and considered important for binding affinity[12g] (Figure 2). The A ring is presumably stabilized by a strong T-shaped arene quadrupole interaction

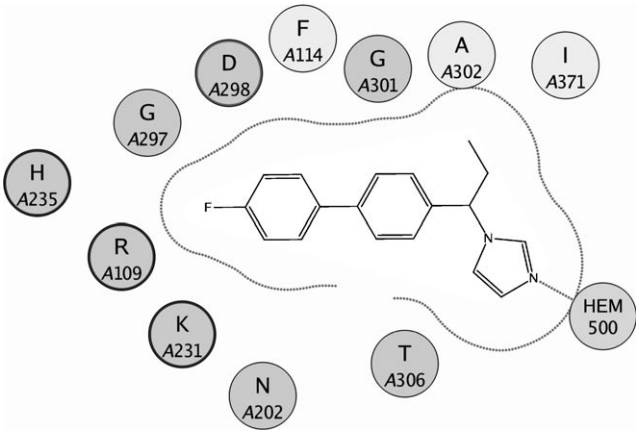

Figure 2. CYP17 residues surrounding **Ref 1**: Arg109 and Lys231 interact with the *para*-fluoro group on the A ring. More amino acids around the A or C rings might form additional multipolar interactions with further fluoro substituents.

with Phe114, a conformationally flexible residue responsible for dividing the CYP17 active site into two lobes. Furthermore, additional amino acid residues such as Asn, Arg, and Gln were observed to be proximal to the A or C rings, and might provide the potential for additional fluorine substituents to form multipolar interactions with H–X (for X = N, O, S),[13h–l] backbone C=O groups (in an orthogonal manner),[13e–f] or even with H–C_α.[13c,g] Consequently, the following strategies to increase the inhibitory potency and metabolic stability of **Ref 1** were applied: a) shifting the fluorine to other positions in the A ring, and b) introduction of additional fluorine atoms on the A or C rings to identify new interaction areas. Because these modifications change the molecular electrostatic potentials (MEPs) of the compounds, the protein pocket surrounding the C ring was scrutinized to identify potential interaction areas influenced by MEP variations, especially the backbone π systems of amino acids such as Gly301–Ala302.

Results and Discussion

Chemistry

The syntheses of compounds **1**–**26** are shown in Schemes 1, 2, and 3. For 1-imidazole analogues **1**–**22**, a general synthetic strategy was employed: ketone or aldehyde intermediates were obtained by Suzuki coupling (Method C) from the corresponding bromides and boronic acids.[14] They were subsequently converted into the alcohols by reduction with $NaBH_4$

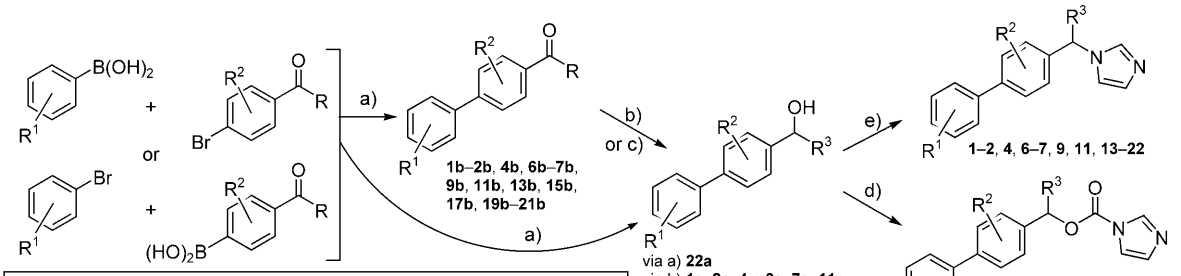

Compd	R^1	R^2	R^3	R	Compd	R^1	R^2	R^3	R
1:	4'-F, 2'-Me	H	Et	Et	**15**:	2',4'-di F	*m*-F	Et	H
2, 3:	3',4'-di F	H	Et	Et	**16**:	2',4'-di F	*m*-F	H	H
4, 5:	2',4'-di F	H	Et	Et	**17**:	2',5'-di F	*m*-F	Et	H
6:	2',4'-di F, 3'-MeO	H	Me	Me	**18**:	2',5'-di F	*m*-F	H	H
7, 8:	2',5'-di F	H	Et	Et	**19**:	4'-F	*o*-F	Et	Et
9, 10:	4'-F	*m*-F	Et	H	**20**:	4'-F	*o*-F	H	H
11, 12:	4'-F	*m*-F	H	H	**21**:	3',4'-di F	*o*-F	Et	Et
13:	3',4'-di F	*m*-F	Et	H	**22**:	2',4'-di F	*o*-F	H	
14:	3',4'-di F	*m*-F	H	H					

Scheme 1. Compounds were synthesized from the corresponding **a** or **b** intermediates unless otherwise indicated. Reagents and conditions: a) Method C: $Pd(PPh_3)_4$, Na_2CO_3, toluene, reflux, 6 h; b) Method D: $NaBH_4$, MeOH; c) Method B: EtMgBr, THF; d) Method E: CDI, THF, reflux, 4 days; e) Method A: CDI, NMP, reflux, 4 h.

(Method D) or Grignard reaction (Method B). The alcohol intermediates reacted with 1,1′-carbonyldiimidazole (CDI) to give racemic mixtures of the desired products, which were not separated into their enantiomers. By varying the reaction conditions such as solvent and temperature, different products were obtained in this S_N2 reaction. After holding at reflux in *N*-methyl-2-pyrrolidone (NMP) for 4 h (Method A),[15] biphenyl methylene imidazoles were obtained, whereas boiling in THF for four days (Method E) gave imidazole-1-carboxylic acid biphenyl esters as major products. Distinguishing between these two products is easy, as the chemical shift values of imidazole 2-H in biphenyl methylene imidazoles are ~7.6 ppm, whereas they are >8.2 ppm in imidazole-1-carboxylic acid biphenyl esters.[15] Moreover, the proton chemical shift of C–H is 5.1 ppm in the biphenyl methylene imidazoles, whereas in the imidazole-1-carboxylic acid biphenyl esters it is 5.9 ppm. Additionally, the strong carbonyl signal in the IR spectra contributes to the identification of the latter class of compounds. For the synthesis of the 5-imidazole analogues **23**–**26** (Schemes 2 and 3), triphenylmethyl (Trt) was employed as the protecting group for imidazole. The alcohol intermediates, commercially available or obtained by reaction of imidazolyl lithium with aldehyde, underwent elimination of the H_2O group under acidic conditions to give the corresponding isopropylidene product, which was subsequently saturated by hydrogenation of the double bond.

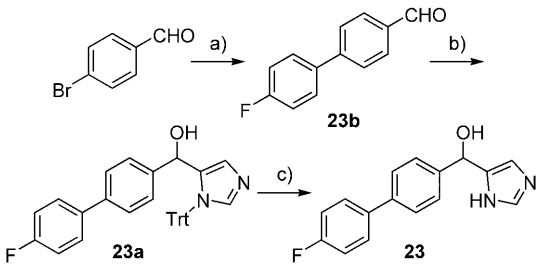

Scheme 2. Reagents and conditions: a) Method C: 4-fluoroboronic acid, $Pd(PPh_3)_4$, Na_2CO_3, toluene, reflux, 6 h; b) 1. imidazole, *n*BuLi, TrtCl, THF, 0 °C, 2 h; 2. *n*BuLi, TBDMSCl, THF, 0 °C, 2 h; 3. *n*Buli, **23b**, THF, room temperature, 8 h; c) pyridinium·HCl, MeOH, 60 °C, 4 h.

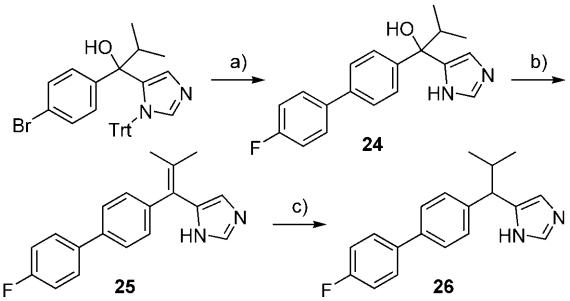

Scheme 3. Reagents and conditions: a) 1. Method C: 4-fluoroboronic acid, $Pd(PPh_3)_4$, Na_2CO_3, toluene, reflux, 6 h; 2. pyridinium·HCl, MeOH, 60 °C, 4 h; b) HCl/*i*PrOH, 80 °C, 2 h; c) $Pd(OH)_2$, EtOH, THF, H_2, room temperature, 3 h.

In vitro activity

CYP17 inhibition of all compounds was evaluated by using the 50 000 *g* sediment after homogenization of *E. coli* expressing human CYP17 as well as cytochrome P450 reductase.[12d] The assay was run with progesterone as substrate and NADPH as cofactor. Separation of substrate and product was carried out by HPLC with UV detection.[16] IC_{50} values are presented in relative to ketoconazole and abiraterone in Tables 1 and 2.

It is striking that in the series of 1-imidazole compounds (**1**–**22**) a sharp structure–activity relationship is observed. The analogues can be divided into three classes based on fluorine substitution on the C ring: without fluoro, *meta*-fluoro, and *ortho*-fluoro (positions relative to the A ring, Table 1). It is apparent that in the class of compounds lacking fluorine at the C ring,

Table 1. Inhibition of CYP17 by compounds **1**–**22**.

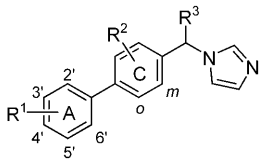

Ref 1, **1**–**2**, **4**, **6**–**7**, **9**, **11**, **13**–**22**

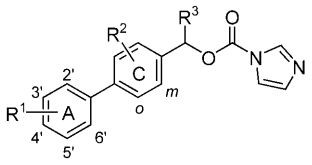

3, **5**, **8**, **10**, **12**

Compd	R^1	R^2	R^3	IC_{50} [nM][a]	Compd	R^1	R^2	R^3	IC_{50} [nM][a]	Compd	R^1	R^2	R^3	IC_{50} [nM][a]
Ref 1	4′-F	H	Et	345	**9**	4′-F	*m*-F	Et	131	19	4′-F	*o*-F	Et	657
					10	4′-F	*m*-F	Et	4643					
					11	4′-F	*m*-F	H	2110	**20**	4′-F	*o*-F	H	2800
					12	4′-F	*m*-F	H	>5000					
1	4′-F, 2′-Me	H	Et	951										
2	3′,4′-diF	H	Et	803	**13**	3′,4′-diF	*m*-F	Et	305	21	3′,4′-diF	*o*-F	Et	825
3	3′,4′-diF	H	Et	>5000	**14**	3′,4′-diF	*m*-F	H	>5000					
4	2′,4′-diF	H	Et	985	**15**	2′,4′-diF	*m*-F	Et	381					
5	2′,4′-diF	H	Et	>5000	**16**	2′,4′-diF	*m*-F	H	>5000	22	2′,4′-diF	*o*-F	H	>5000
6	2′,4′-diF, 3′-MeO	H	Me	>10000										
7	2′,5′-diF	H	Et	956	**17**	2′,5′-diF	*m*-F	Et	364					
8	2′,5′-diF	H	Et	>5000	**18**	2′,5′-diF	*m*-F	H	1640					
KTZ[b]				2780						ABT[b]				72

[a] Compound concentration required to give 50% inhibition; values represent the mean ±10% deviation of at least three experiments. [b] KTZ: ketoconazole, ABT: abiraterone.

additional substitution at the A ring by fluoro, methyl, or methoxy groups (**1**, **2**, **4**, **6**, and **7**), does not enhance the inhibitory activity relative to **Ref 1** (IC_{50} = 345 nM). For example, extra fluorine substitution at the *meta* or *ortho* positions of the A ring, resulting in 3′,4′-difluoro analogue **2** and 2′,4′-difluoro analogue **4**, decreased activity somewhat (IC_{50}: 803 and 985 nM, respectively). Interestingly, 2′,5′-difluoro substitution (compound **7**) resulted in similar inhibitory potency (IC_{50} = 956 nM) as observed with the 2′,4′-difluoro analogue.

Importantly, the introduction of fluorine at the *meta* position of the C ring significantly increases inhibitory potency. Compound **9** has an IC_{50} value of 131 nM, being threefold more potent than **Ref 1**. Similar improvements can be found for the other compounds in this class (**13**, **15**, and **17**; IC_{50} values ~350 nM), which are threefold more potent than the corresponding compounds without fluoro group substitution at the C ring (**2**, **4**, and **7**, respectively; IC_{50} values ~900 nM). Moreover, the analogue with only one *para*-fluoro substituent at the A ring (compound **9**) is more potent than other analogues with multiple fluorine atoms on the A ring, as mentioned above. A similar potency ranking is observed for polyfluorinated analogues in this compound class as well: the 3′,4′-difluoro compound **13** (IC_{50} = 305 nM) is more potent than the others: for example, the 2′,5′-difluoro compound **15** (IC_{50} = 381 nM) and the 2′,4′-difluoro compound **17** (IC_{50} = 364 nM).

In contrast, *ortho*-fluoro substitution at the C ring decreases activity. Compound **19** (IC_{50} = 657 nM) is less potent than the corresponding analogues with *meta*-fluoro groups (compound **9**, IC_{50} = 131 nM) or those lacking fluorine (**Ref 1**, IC_{50} = 345 nM). However, compound **19** exhibited stronger inhibition than compound **21**, which bears two fluorine substituents at the 3′ and 4′ positions, as expected.

Moreover, all imidazole-1-carboxylic acid biphenyl esters (**3**, **5**, **8**, **10**, and **12**), which have been shown by HPLC to be stable in incubation buffer, were found to be inactive. This is probably due to the fact that these compounds are too large to fit into the binding pocket. Notably, the ethyl substituent at the methylene bridge is important, as previously reported;[12g] that is, ethyl substitution results in compounds that are more potent than the corresponding unsubstituted or methyl-substituted analogues.

Furthermore, 5-imidazole was employed instead of 1-imidazole, leading to compounds **23**–**26** as shown in Table 2. It is apparent that compounds with a hydroxy group substituted at the methylene bridge are inactive. Nonetheless, isopropyl substitution resulted in an active compound (**26**, IC_{50} = 502 nM) which was, however, less potent than **Ref 1**. Surprisingly, com-

Table 2. Inhibition of CYP17 by compounds **23**–**26**.

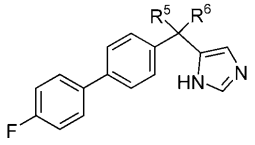

Compd	R^5	R^6	IC_{50} [nM][a]
23	OH	H	≫10000
24	OH	*i*Pr	>5000
25	isopropylidene		159
26	H	*i*Pr	502
KTZ[b]			2780
ABT[b]			72

[a] Compound concentration required to give 50% inhibition; values represent the mean ±10% deviation of at least three experiments. [b] KTZ: ketoconazole, ABT: abiraterone.

pound **25**, with an isopropylidene substitution, turned out to be very potent ($IC_{50} = 159$ nM).

Finally, inhibition values of the most active compounds **9**, **13**, **15**, **17**, and **25** toward the hepatic enzyme CYP3A4 were also determined because of its important role in drug metabolism and drug–drug interactions. It turned out that the compounds tested showed only marginal inhibition (~50% at 10 μM), clearly lower than that shown by ketoconazole (98% at 10 μM).

Computational studies

Docking

Compounds **Ref 1**, **9**, **11**, **13**, **15**, **17**, and **19**, both enantiomers if present, were docked into the homology model of human CYP17[12e] by means of two commercial docking software packages, GOLD_v. 4.0[17] and FlexX 3.1.3,[18] in order to elucidate their binding into the active site of the enzyme. Docking with GOLD was performed with both the scoring functions GoldScore and ChemScore, while FlexX was used with the FlexX-Pharm module, with the iron center of the heme chosen as pharmacophoric constraint. A clustering with ACIAP[19] of all the docking poses of the three procedures resulted in one main statistically predominant binding mode (BM1)[12e] and two minor representative clusters. Interestingly, each of the latter two clusters consisted solely of either the *S* (BM2)[12e] or the *R* (BM-ABT)[12h] enantiomers (Figure 3). This finding indicates that, together with the necessary perpendicular interaction angle between imidazole N and heme Fe to ensure sufficient coordination, the orientation of the hydrophobic pocket, which is occupied by the substituent on the methylene bridge, limits the pose distribution of different enantiomers. This geometrical restriction forces the *S* enantiomers into the BM2 area and the *R* enantiomers into BM-ABT. However, as the intersection of both areas, BM1 is a better area for both enantiomers to bind.

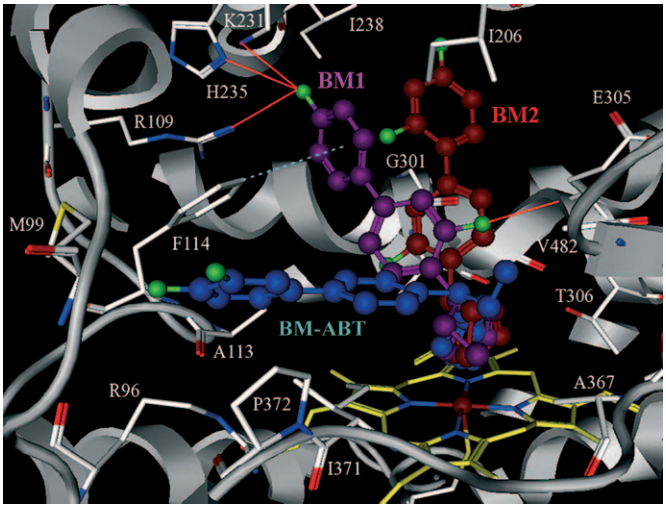

Figure 3. Presentation of the three main binding modes exemplified by compounds **9** (magenta, BM1), **15** (red, BM2) and **13** (blue, BM-ABT). Here, interacting residues and the tertiary structure (ribbon) of the active site are shown. Polar interactions are marked with red solid lines, whereas π–π stacking and metal complexation are indicated with cyan dotted lines. This image was generated with MOE (http://www.chemcomp.com).

It was observed for BM1 that a conjugated scaffold oriented almost parallel to the I-helix is one of the key factors for high activity, as previously described.[12g] According to our docking studies this extended π system clearly interacts not only with the π system of the amino acid backbone in the I-helix (i.e., Gly301, Ala302, Gly303, and Val304), but also with Phe114, which is oriented perpendicular to the A ring (Figure 3, BM1) to form a quadrupole–quadrupole interaction. More importantly, fluorine in the molecule showed profound influence on the affinity for the enzyme. This can be explained by the clear interactions of the *para*-fluoro substituent with Arg109, Lys231, and His235 (Figure 3). When the fluorine atoms were shifted to other positions in the A ring resulting in 2′,5′-difluoro analogues, a decrease in activity can be observed. Clearly, the interactions mentioned above can no longer be maintained. These observations nicely validate the reliability of our protein model. Furthermore, the elevated activity of C ring *meta*-fluoro-substituted compounds can be explained by a multipolar interaction between F and the N–H group of Glu305 (Figure 3) stabilizing the π–π interaction between the C ring and the backbone π system of Gly301–Ala302.

Additionally, a further flexible docking run was performed with GOLD v. 4.0–GoldScore, with the side chains of Phe114, Arg109, Lys231, Asn202, Glu305, and Ile371 being set as freely rotatable. Very similar results were observed as those for the docking runs with the rigid side chains (data not shown).

MEP maps

To gain insight into which physicochemical parameters might influence biological activity, the charge density distribution was considered, and the molecular electrostatic potentials of selected compounds were determined. The geometry of these compounds (**Ref 1**, **2**, **9**, **13**, **15**, **17**, and **25**) was optimized in the gas phase at the B3LYP/6-311++G** (d,p)[20] level of density functional theory (DFT) by means of Gaussian 03.[21] MEPs of electron density were plotted for every compound with GaussView 3.09.[22]

The introduction of a second fluorine or the shift of fluorine into another position on the A ring always leads to a decrease in A ring electron density, which can be clearly observed in the various MEP maps of compounds **9**, **13**, **15**, **17**, and **25** (Figure 4 A). This observation correlates with the different electron-withdrawing effects of the fluorine atom in the *meta* or *para* position (σ values of +0.337 and +0.067, respectively). This decrease in electron density weakens the T-shaped interaction of the A ring with Phe114, and consequently decreases the inhibitory potency of the compound.

The lower inhibitory potency of compounds with *ortho*-fluoro substitution on the C ring (compounds **19** and **21**) might be due to the adverse effect that the fluorine exerts on the overall charge density of the biphenyl system by deforming the conjugated π–π system and by concentrating the electrons on the fluorine. However, for *meta*-fluoro compounds **9**,

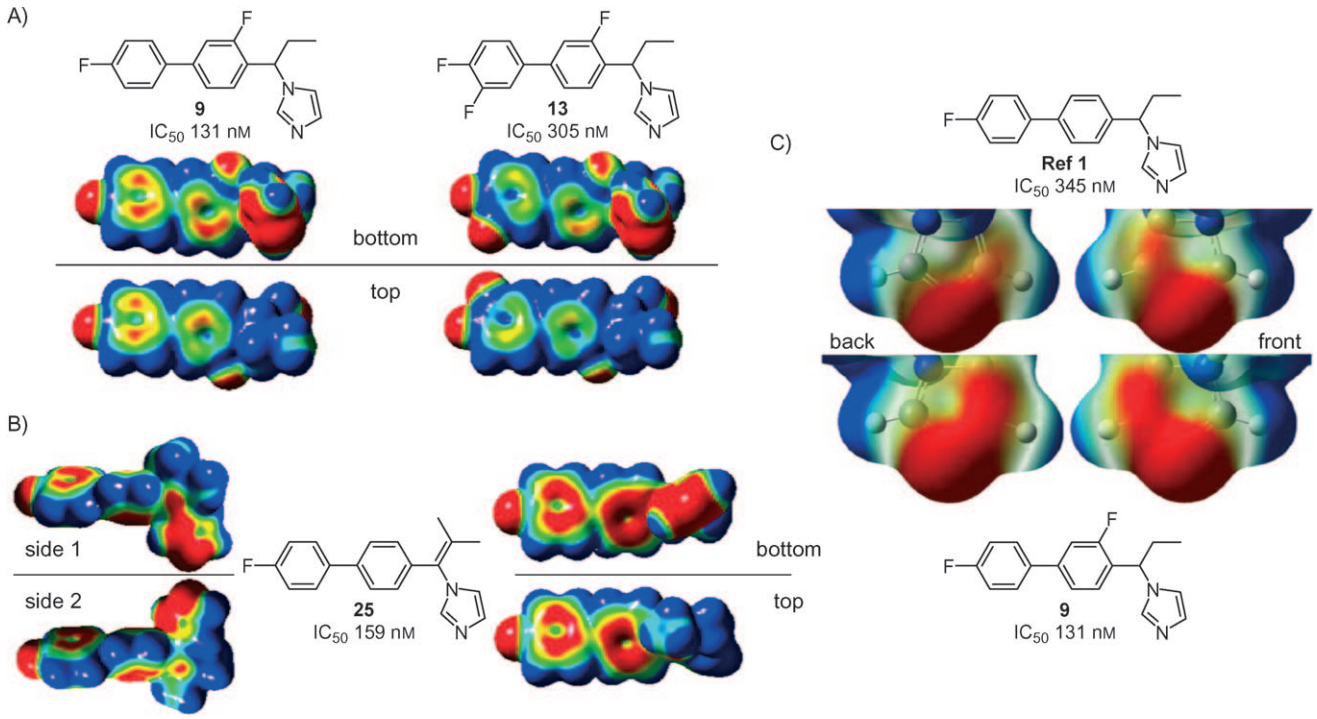

Figure 4. A) Structure, CYP17 inhibitory activity, and MEP maps (bottom and top view) of compounds **9** and **13**. For compounds **15** and **17**, nearly the same MEP maps (not shown) as for compound **13** were observed. B) MEP maps of compound **25**, highlighting the side views of the conjugated π–π system enhanced by the isopropylidene substituent on the methylene bridge. The electrostatic potential surfaces shown in A) and B) were plotted with GaussView 3.0 in a range of −6 to +12 kcal mol^{-1}. C) Transparent color-coded front and back view of the electrostatic potential maps of the imidazole groups of both **Ref 1** and compound **9**, in a range of −15.7 to +0 kcal mol^{-1}, illustrating the influence exerted on the electron distribution of the imidazole by fluorine substituents on the C ring.

13, **15**, and **17**, it seems that fluorine induces an increase in electron distribution on the imidazole ring, as visualized in the MEP maps of compounds **Ref 1** and **9** (Figure 4C), which is associated with an augmented inhibitory potency of the compounds. An analogous phenomenon was observed for compound **25**, in which the isopropylidene group strengthens the π–π system and extends the conjugation over the whole molecule (Figure 4B).

In vivo activity

The in vivo evaluation of the most potent compounds **9**, **13**, **15**, and **17**, including the ability to decrease plasma testosterone concentrations (Figure 5) and the determination of pharmacokinetic properties (Table 3), was performed in male Wistar rats after oral application. Abiraterone, which was administered in its acetate form to improve oral absorption, and **Ref 1** were used as reference compounds. The plasma concentrations of testosterone were determined using an ELISA assay, and plasma drug concentrations were measured by LC–MS. In the case of abiraterone acetate, only the signals of free abiraterone were monitored, as the acetate is inactive as a CYP17 inhibitor. As can be seen in Figure 5, all compounds significantly decreased the plasma testosterone concentration. It is striking at each time point investigated that all nonsteroidal compounds, which were less active in vitro, exhibited higher activities in vivo than abiraterone. After 24 h, compound **9** and **Ref 1** still showed strong inhibitory activity, compounds **13** and **17** showed almost no inhibition, and compound **15** and abiraterone exhibited an increase in testosterone levels above control at this time point, probably caused by feedback stimulation. As expected, this activity profile correlates to the pharmacokinetic properties of the compounds. Abiraterone exhibited a plasma half-life of only 1.6 h, while the half-lives of other compounds are much longer (10 h for **Ref 1** and 12.8 h for **9**). Accordingly, the AUC values of the test compounds, except for compound **17**, are higher than that of abiraterone, indicating better bioavailability. Interestingly, the introduction of an addi-

Table 3. Pharmacokinetic properties of selected compounds.[a]

Compd	$t_{1/2,z}$ [h][b]	t_{max} [h][c]	C_{max} [nM][d]	C_{24h} [nM][e]	$AUC_{0-\infty}$ [nM h^{-1}][f]
9	12.8	2.0	3473	1528	80448
13	6.1	8.0	3496	1173	56114
15	4.2	6.0	2539	556	35091
17	2.2	1.0	458	187	2055
Ref 1	10.0	6.0	11729	4732	252297
ABT	1.6	2.0	1694	253	11488

[a] Compounds **Ref 1**, **9**, **13**, **15**, and **17** were applied at a dose of 50 mg kg^{-1}; abiraterone (ABT) was administrated as abiraterone acetate (56 mg kg^{-1}, equivalent to ABT 50 mg kg^{-1}). Five to six intact adult male Wistar rats were employed for each treatment group; each sample was tested three times. [b] Terminal half-life. [c] Time of maximal concentration. [d] Maximal concentration. [e] Concentration at 24 h. [f] Area under the curve.

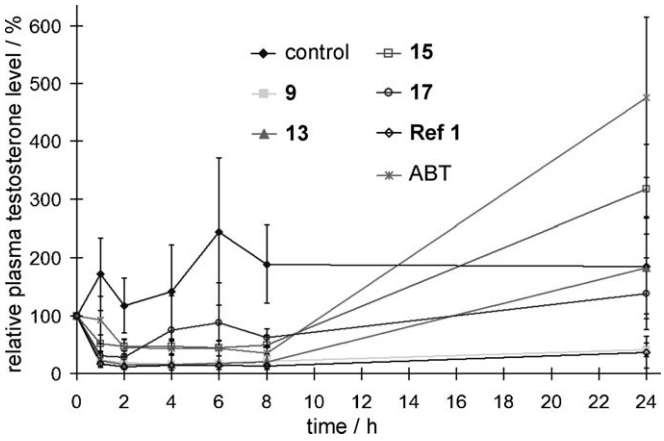

Figure 5. Reduction of plasma testosterone concentrations in rats by selected compounds. Compounds **Ref 1**, **9**, **13**, **15**, and **17** were applied at a dose of 50 mg kg^{-1}; abiraterone (ABT) was administrated as abiraterone acetate (56 mg kg^{-1}, equivalent to abiraterone at 50 mg kg^{-1}). Five to six intact adult male Wistar rats were employed for each treatment group; each sample was tested three times. The average plasma testosterone concentrations (1.97 ng mL^{-1}) at pre-treatment time points (−1, −0.5 and 0 h) were set at 100%. The values shown are relative to the pre-treatment value.

tional fluorine into the C ring of **Ref 1** prolongs plasma half-life (compound **9**), whereas introduction of further fluorine atoms into the A ring significantly decreases half-life values (**13**, **15**, and **17**; $t_{1/2}$: 2–6 h). This is probably due to the electron-withdrawing effects of multiple fluoro group substitution. Fluorine atoms significantly weaken the adjacent aromatic C–H bonds, making them more vulnerable to nucleophilic attack.[13m]

Conclusions

Herein we report the design, synthesis, and bioactivity evaluation of a series of fluorine-substituted biphenyl methylene imidazoles as CYP17 inhibitors. Fluorine substitution showed a profound influence on the in vitro and in vivo activities, as well as the pharmacokinetic profiles.

We observed that fluorine at the *meta* position of the C ring increases activity relative to unsubstituted analogues, whereas *ortho* substitution decreases potency. Compounds bearing fluorine at the A ring consistently follow the same activity ranking: 4′-F > 3′,4′-di F > 2′,5′-di F ≥ 2′,4′-di F. Although the compounds are racemates, it is not likely that one enantiomer would be much more potent than the other, because both *S* and *R* enantiomers predominately adopt BM1 according to our docking studies. Close inspection of the docking poses reveals that the biphenyl moieties of both enantiomers are placed in the same area, interacting with Arg109 and Lys231, and the positioning of their imidazolyl methylene groups exhibits only a slight difference. The conformational flexibility of the imidazolyl methylene group allows the ethyl substituents of both enantiomers to orient toward the hydrophobic pocket that is opposite to the I-helix and delimited by Ile371 and Ala367. Moreover, the biological data were well deciphered by docking studies and MEP mapping of selected compounds. The multipolar interactions between the C ring fluorine substituents and interacting amino acid residues significantly increased the binding affinities relative to the parent compound. The charge distribution difference on both the A and C rings indicates π–π stacking (i.e., with both Phe114 and Gly301–Ala302), hydrophobic, and van der Waals interactions as determinants for activity. Furthermore, it was demonstrated once again that fluorine substituted in an appropriate position, like in the C ring, prolongs the plasma half-life; in an unsuitable position, however, it decreases the $t_{1/2\,z}$ value of the parent compound. This phenomenon might be due to a decrease in metabolic stability and is an interesting subject for future investigations.

Finally, after the modification, compound **9** was identified as a strong CYP17 inhibitor showing potent activity in vivo, high bioavailability, and a long plasma half-life. Thus, compound **9** appears to be an optimal candidate, which, after further structural optimization, could be the first nonsteroidal CYP17 inhibitor to be applied clinically. CYP17 inhibitors are expected to be superior to the GnRH analogues in current use as mentioned above, because they decrease not only testicular but also adrenal androgen formation. Nevertheless, PC treatment could be further optimized by combining CYP17 inhibitors with inhibitors of androgen activation to DHT, catalyzed by 17β-HSD1[23] and/or 17β-HSD3, as well as 5αR.[24]

Experimental Section

CYP17 preparation and assays

Human CYP17 was expressed in *E. coli* (co-expressing human CYP17 and cytochrome P450 reductase), and the assay was performed as previously described.[12d,16]

Inhibition of hepatic CYP enzyme

The recombinantly expressed enzyme from baculovirus-infected insect microsome (Supersome) was used, and the manufacturer's instructions (http://www.gentest.com) were followed.

In vivo studies

The in vivo tests were performed with intact adult male Wistar rats (Harlan Winkelmann, Germany), five to six for each treatment group. These rats were cannulated with silicone tubing via the right jugular vein. Compounds **9**, **13**, **15**, and **17** were applied p.o. at doses of 50 mg kg^{-1}, while abiraterone was administrated as the acetate at 56 mg kg^{-1} (equivalent to abiraterone at 50 mg kg^{-1}). The concentrations of testosterone in the rat plasma were determined by ELISA (EIA-1559) from DRG Instruments according to the manufacturer's instructions. The plasma drug levels were measured by LC–MS. Non-compartmental pharmacokinetic analysis of concentration versus time was performed for each compound on the mean plasma level using a validated computer program (PK solution 2 software, Summit Research Services, Montrose, CO, USA). Plasma concentrations below the limit of detection were assigned a value of zero.

Chemistry

General: Melting points were determined on a Mettler FP1 melting point apparatus and are uncorrected. IR spectra were recorded

neat on a Bruker Vector 33 FTIR spectrometer. ^{1}H and ^{13}C NMR spectra were measured on a Bruker DRX-500 (500 MHz). Chemical shifts (δ) are given in parts per million (ppm), and $(CH_3)_4Si$ was used as an internal standard for spectra obtained. All coupling constants (J) are given in Hz. ESI (electrospray ionization) mass spectra were determined on a TSQ Quantum (Thermo Electron Corporation) instrument. High-resolution mass spectra were measured using an LTQ Orbitrap (Thermo Electron Corporation) with positive ESI. The purities of the final compounds were determined by a Surveyor LC system and were >98%. Column chromatography was performed using silica gel 60 (50–200 μm), and reaction progress was monitored by TLC on Alugram SIL G/UV$_{254}$ (Macherey–Nagel). Boronic acids and bromoaryl compounds used as starting materials were commercially obtained (CombiBlocks, Chempur, Aldrich, Acros, etc).

Method A: CDI reaction in NMP. CDI (5 equiv) was added to a solution of the corresponding alcohol (1 equiv) in NMP or CH_3CN (10 mL mmol^{-1}). The solution was then heated at reflux for 4–18 h. After cooling to room temperature, it was diluted with H_2O (30 mL) and extracted with EtOAc (3×10 mL). The combined organic phases were washed with brine, dried over $MgSO_4$ and evaporated under reduced pressure. The desired product was then purified by chromatography on silica gel.

1-[1-(4′-Fluoro-2′-methylbiphenyl-4-yl)propyl]-1*H*-imidazole (1). Synthesized according to Method A using **1a** (0.15 g, 0.61 mmol) and CDI (0.20 g, 1.23 mmol); yield: 0.06 g (32%); colorless oil; R_f= 0.27 (CH_2Cl_2/MeOH, 95:5); ^{1}H NMR (DMSO, 500 MHz): δ=0.98 (t, J=7.3 Hz, 3H, CH_3), 2.23 (s, 3H, CH_3), 2.24–2.30 (m, 2H, CH_2), 5.07 (t, J=7.6 Hz, 1H, CH), 6.90–6.93 (m, 1H), 6.95–6.97 (m, 1H), 7.01 (s, 1H), 7.11 (s, 1H), 7.14 (dd, J=6.0, 8.4 Hz, 1H), 7.22–7.26 (m, 4H), 7.67 ppm (s, 1H); ^{13}C NMR ([D$_6$]DMSO, 125 MHz): δ=11.1 (CH_3), 20.5 (CH_3), 28.6 (CH_2), 63.2 (CH), 112.5, 112.6, 116.7, 116.9, 126.3, 129.7, 131.1, 131.1, 137.0, 137.6, 137.7, 138.9, 140.9, 161.1, 163.0 ppm; HRMS (ESI): calcd for $C_{19}H_{20}FN_2$ $[M+H]^+$: 295.1611, found: 295.1607; MS (ESI): m/z=295 $[M+H]^+$.

1-[1-(3′,4′-Difluorobiphenyl-4-yl)propyl]-1*H*-imidazole (2). Synthesized according to Method A using **2a** (0.27 g, 1.09 mmol) and CDI (0.34 g, 2.06 mmol); yield: 0.09 g (27%); colorless oil; R_f=0.29 (CH_2Cl_2/MeOH, 95:5); ^{1}H NMR ($CDCl_3$, 500 MHz): δ=0.98 (t, J=7.3 Hz, 3H, CH_3), 2.23–2.31 (q, J=7.3, 7.6 Hz, 2H, CH_2), 5.06 (t, J=7.6 Hz, 1H, CH), 6.97–7.02 (m, 1H), 7.10–7.14 (m, 1H), 7.18–7.28 (m, 4H), 7.23–7.37 (m, 1H), 7.49 (m, 2H), 7.62–7.66 ppm (m, 1H, Im-2H); ^{13}C NMR ($CDCl_3$, 125 MHz): δ=11.3 (CH_3), 29.6 (CH_2), 63.0 (CH), 116.3, 117.5, 118.7, 123.2, 127.3, 130.5, 136.5, 137.4, 140.5, 151.3 ppm; HRMS (ESI): calcd for $C_{18}H_{17}F_2N_2$ $[M+H]^+$: 299.1360, found: 299.1363; MS (ESI): m/z=299 $[M+H]^+$.

1-[1-(2′,4′-Difluorobiphenyl-4-yl)propyl]-1*H*-imidazole (4). Synthesized according to Method A using **4a** (0.27 g, 1.09 mmol) and CDI (0.34 g, 2.06 mmol); yield: 0.12 g (36%); colorless oil; R_f=0.34 (CH_2Cl_2/MeOH, 95:5); ^{1}H NMR ($CDCl_3$, 500 MHz): δ=0.85 (t, J=7.3 Hz, 3H, CH_3), 2.12–2.18 (m, 2H, CH_2), 4.96 (t, J=7.6 Hz, 1H, CH), 6.77–6.85 (m, 2H), 6.87–6.90 (m, 1H), 6.99–7.02 (m, 1H), 7.13–7.15 (m, 2H), 7.23–7.28 (m, 1H), 7.35–7.37 (m, 2H), 7.62–7.68 ppm (m, 1H, Im-2H); ^{13}C NMR ($CDCl_3$, 125 MHz): δ=11.1 (CH_3), 29.3 (CH_2), 63.3 (CH), 104.5, 112.7, 117.8, 118.6, 124.6, 126.3, 130.2, 131.4, 135.7, 136.6, 140.3, 163.5 ppm; HRMS (ESI): calcd for $C_{18}H_{17}F_2N_2$ $[M+H]^+$: 299.1360, found: 299.1352; MS (ESI): m/z=299 $[M+H]^+$.

1-[1-(2′,4′-Difluoro-3′-methoxybiphenyl-4-yl)ethyl]-1*H*-imidazole (6). Synthesized according to Method A using **6a** (0.30 g, 1.09 mmol) and CDI (0.34 g, 2.06 mmol); yield: 0.34 g (71%); yellow oil; R_f=0.30 (CH_2Cl_2/MeOH, 95:5); ^{1}H NMR ($CDCl_3$, 500 MHz): δ=1.75 (d, J=7.5 Hz, 3H, CH_3), 3.91 (s, 3H, OCH_3), 5.18–5.31 (q, J=7.5 Hz, 1H, CH), 6.82–6.83 (m, 1H), 6.84–6.86 (m, 1H), 6.89–6.93 (m, 1H), 6.97–6.99 (m, 1H), 7.09–7.10 (m, 2H), 7.34–7.36 (m, 2H), 7.50–7.51 ppm (m, 1H, Im-2H); ^{13}C NMR ($CDCl_3$, 125 MHz): δ=21.1 (CH_3), 56.7 (CH), 62.5 (OCH_3), 112.3, 117.7, 123.9, 125.6, 127.8, 128.4, 134.1, 136.1, 141.6 ppm; HRMS (ESI): calcd for $C_{18}H_{17}F_2N_2O$ $[M+H]^+$: 315.1309, found: 315.1297; MS (ESI): m/z=315 $[M+H]^+$.

1-[1-(2′,5′-Difluorobiphenyl-4-yl)propyl]-1*H*-imidazole (7). Synthesized according to Method A using **7a** (0.27 g, 1.09 mmol) and CDI (0.34 g, 2.06 mmol); yield: 0.13 g (41%); colorless oil; R_f=0.38 (CH_2Cl_2/MeOH, 95:5); ^{1}H NMR ($CDCl_3$, 500 MHz): δ=0.98 (t, J=7.3 Hz, 3H, CH_3), 2.26 (q, J=7.3, 7.6 Hz, 2H, CH_2), 5.05 (t, J=7.6 Hz, 1H, CH), 6.97–7.01 (m, 2H), 7.08–7.12 (m, 3H), 7.25–7.27 (m, 2H), 7.49–7.51 (m, 2H), 7.62–7.65 ppm (m, 1H, Im-2H); ^{13}C NMR ($CDCl_3$, 125 MHz): δ=11.3 (CH_3), 29.6 (CH_2), 63.1 (CH), 116.8, 118.4, 126.5, 130.5, 135.4, 136.9, 140.0, 158.8, 160.7 ppm; HRMS (ESI): calcd for $C_{18}H_{17}F_2N_2$ $[M+H]^+$: 299.1360, found: 299.1351; MS (ESI): m/z=299 $[M+H]^+$.

1-[1-(3,4′-Difluorobiphenyl-4-yl)propyl]-1*H*-imidazole (9). Synthesized according to Method A using **9a** (0.38 g, 1.53 mmol) and CDI (0.47 g, 2.88 mmol); yield: 0.08 g (17%); yellow oil; R_f=0.38 (CH_2Cl_2/MeOH, 95:5); ^{1}H NMR ($CDCl_3$, 500 MHz): δ=0.99 (t, J=7.3 Hz, 3H, CH_3), 2.21–2.31 (m, 2H, CH_2), 5.38 (t, J=7.5 Hz, 1H, CH), 7.01 (s, 1H), 7.08 (s, 1H), 7.10–7.14 (m, 2H), 7.19–7.25 (m, 2H), 7.27–7.29 (m, 1H), 7.40–7.51 (m, 2H), 7.64 ppm (s, 1H, Im-2H); ^{13}C NMR ($CDCl_3$, 125 MHz): δ=11.3 (CH_3), 28.6 (CH_2), 56.4 (CH), 114.5, 116.3, 118.0, 123.7, 126.6, 127.3, 128.9, 129.5, 130.9, 135.0, 136.5, 161.7, 163.4 ppm; ^{19}F NMR ($CDCl_3$, 400 MHz): δ=−114.19 (s, 1F), −117.98 ppm (s, 1F); HRMS (ESI): calcd for $C_{18}H_{17}F_2N_2$ $[M+H]^+$: 299.1360, found: 299.1352; MS (ESI): m/z=299 $[M+H]^+$.

1-[(3,4′-Difluorobiphenyl-4-yl)methyl]-1*H*-imidazole (11). Synthesized according to Method A using **11a** (0.28 g, 1.27 mmol) and CDI (0.41 g, 2.54 mmol); yield: 0.11 g (31%); colorless oil; R_f=0.53 (EtOAc/MeOH, 95:5); ^{1}H NMR ($CDCl_3$, 500 MHz): δ=5.20 (s, 2H, CH_2), 6.98 (br s, 1H), 7.10 (br s, 1H), 7.11–7.16 (m, 3H), 7.26–7.31 (m, 2H), 7.50 (dd, J=5.4, 8.8 Hz, 2H), 7.64 ppm (br s, 1H, Im-2H); ^{13}C NMR ($CDCl_3$, 125 MHz): δ=44.4 (CH_2), 114.2, 115.9, 119.2, 122.2, 123.1, 128.6, 129.6, 129.9, 135.3, 137.3, 142.9, 160.6, 162.9 ppm; HRMS (ESI): calcd for $C_{16}H_{13}F_2N_2$ $[M+H]^+$: 271.1047, found: 271.1039; MS (ESI): m/z=271 $[M+H]^+$.

1-[1-(3,3′,4′-Trifluorobiphenyl-4-yl)propyl]-1*H*-imidazole (13). Synthesized according to Method A using **13a** (0.40 g, 1.70 mmol) and CDI (0.53 g, 3.20 mmol); yield: 0.11 g (20%); colorless oil; R_f=0.35 (CH_2Cl_2/MeOH, 95:5); ^{1}H NMR ($CDCl_3$, 500 MHz): δ=0.99 (t, J=7.3 Hz, 3H, CH_3), 2.22–2.33 (m, 2H, CH_2), 5.39 (t, J=7.6 Hz, 1H, CH), 7.01 (s, 1H), 7.09 (s, 1H), 7.20–7.29 (m, 5H), 7.31–7.35 (m, 1H), 7.64 ppm (s, 1H, Im-2H); ^{13}C NMR ($CDCl_3$, 125 MHz): δ=11.3 (CH_3), 28.6 (CH_2), 56.3 (CH), 114.5, 116.2, 118.4, 123.9, 127.5, 128.3, 130.5, 136.7, 149.4, 161.7 ppm; ^{19}F NMR ($CDCl_3$, 400 MHz): δ=−117.56 (s, 1F), −136.80 (d, $^3J_{FF}$=−20.7, 1F), −138.64 ppm (d, $^3J_{FF}$=−20.7, 1F); HRMS (ESI): calcd for $C_{18}H_{16}F_3N_2$ $[M+H]^+$: 317.1266, found: 317.1257; MS (ESI): m/z=317 $[M+H]^+$.

1-[(3,3′,4′-Trifluorobiphenyl-4-yl)methyl]-1*H*-imidazole (14). Synthesized according to Method A using **14a** (0.35 g, 1.67 mmol) and CDI (0.53 g, 3.20 mmol); yield: 0.10 g (23%); white powder, mp: 60–61 °C; R_f=0.26 (CH_2Cl_2/MeOH, 95:5); ^{1}H NMR ($CDCl_3$, 500 MHz): δ=5.19 (s, 2H, CH_2), 6.97 (s, 1H), 7.10 (s, 1H), 7.11–7.14 (m, 2H), 7.20–7.28 (m, 3H), 7.31–7.35 (m, 1H), 7.59 ppm (s, 1H, Im-2H); ^{13}C NMR ($CDCl_3$, 125 MHz) 44.3 (CH_2), 114.9, 116.4, 118.6, 119.3, 123.9, 129.5, 136.8, 137.3, 141.4, 149.3, 151.7, 161.4 ppm; HRMS

(ESI): calcd for $C_{16}H_{12}F_3N_2$ $[M+H]^+$: 289.0953, found: 289.0944; MS (ESI): $m/z = 289$ $[M+H]^+$.

1-[1-(2′,3,4′-Trifluorobiphenyl-4-yl)propyl]-1*H*-imidazole (15). Synthesized according to Method A using **15a** (0.27 g, 1.14 mmol) and CDI (0.35 g, 2.10 mmol); yield: 0.09 g (24%); colorless oil; $R_f = 0.37$ (CH_2Cl_2/MeOH, 95:5); ^{1}H NMR ($CDCl_3$, 500 MHz): $\delta = 0.99$ (t, $J = 7.3$ Hz, 3H, CH_3), 2.23–2.32 (m, 2H, CH_2), 5.40 (t, $J = 7.6$ Hz, 1H, CH), 6.89–6.97 (m, 2H), 7.02 (s, 1H), 7.08 (s, 1H), 7.19–7.27 (m, 3H), 7.34–7.38 (m, 1H), 7.64 ppm (s, 1H, Im-2H); ^{13}C NMR ($CDCl_3$, 125 MHz): $\delta = 11.3$ (CH_3), 27.7 (CH_2), 56.2 (CH), 104.5, 112.7, 116.9, 117.7, 125.4, 127.0, 130.8, 136.5, 137.9, 160.3, 161.2 ppm; ^{19}F NMR ($CDCl_3$, 400 MHz): $\delta = -109.86$ (d, $^4J_{FF} = 8.0$, 1F), −113.15 (d, $^4J_{FF} = 8.0$, 1F), −118.03 ppm (s, 1F); HRMS (ESI): calcd for $C_{18}H_{16}F_3N_2$ $[M+H]^+$: 317.1266, found: 317.1257; MS (ESI): $m/z = 317$ $[M+H]^+$.

1-[(2′,3,4′-Trifluorobiphenyl-4-yl)methyl]-1*H*-imidazole (16). Synthesized according to Method A using **16a** (0.18 g, 0.76 mmol) and CDI (0.24 g, 1.51 mmol); yield: 0.09 g (42%); orange oil; $R_f = 0.52$ (EtOAc/MeOH, 95:5); ^{1}H NMR ($CDCl_3$, 500 MHz): $\delta = 5.20$ (s, 2H, CH_2), 6.89–6.97 (m, 2H), 6.98 (brs, 1H), 7.10 (brs, 1H), 7.12 (dd, $J = 7.9$, 8.2 Hz, 1H), 7.24–7.27 (m, 2H), 7.36 (ddd, $J = 6.4$, 8.5, 8.8 Hz, 1H), 7.61 ppm (brs, 1H, Im-2H); ^{13}C NMR ($CDCl_3$, 125 MHz): $\delta = 44.3$ (CH_2), 104.6, 111.8, 116.2, 119.2, 122.8, 123.3, 125.1, 129.4, 129.8, 131.1, 137.4, 159.2, 159.6, 161.2, 162.7 ppm; HRMS (ESI): calcd for $C_{16}H_{12}F_3N_2$ $[M+H]^+$: 289.0953, found: 289.0952; MS (ESI): $m/z = 289$ $[M+H]^+$.

1-[1-(2′,3,5′-Trifluorobiphenyl-4-yl)propyl]-1*H*-imidazole (17). Synthesized according to Method A using **17a** (0.40 g, 1.70 mmol) and CDI (0.53 g, 3.20 mmol); yield: 0.14 g (26%); colorless oil; $R_f = 0.38$ (CH_2Cl_2/MeOH, 95:5); ^{1}H NMR ($CDCl_3$, 500 MHz): $\delta = 0.99$ (t, $J = 7.3$ Hz, 3H, CH_3), 2.23–2.32 (m, 2H, CH_2), 5.40 (t, $J = 7.6$ Hz, 1H, CH), 7.00–7.04 (m, 2H), 7.08–7.14 (m, 2H), 7.20–7.24 (m, 1H), 7.26–7.30 (m, 2H), 7.64 ppm (s, 1H, Im-2H); ^{13}C NMR ($CDCl_3$, 125 MHz): $\delta = 11.3$ (CH_3), 27.6 (CH_2), 56.3 (CH), 116.7, 117.9, 125.5, 127.0, 130.3, 136.7, 158.5, 159.7, 161.4 ppm; ^{19}F NMR ($CDCl_3$, 400 MHz): $\delta = -117.81$ (s, 1F), −118.39 (d, $^5J_{FF} = 17.7$, 1F), −123.67 ppm (d, $^5J_{FF} = 17.7$, 1F); HRMS (ESI): calcd for $C_{18}H_{16}F_3N_2$ $[M+H]^+$: 317.1266, found: 317.1257; MS (ESI): $m/z = 317$ $[M+H]^+$.

1-[(2′,3,5′-Trifluorobiphenyl-4-yl)methyl]-1*H*-imidazole (18). Synthesized according to Method A using **18a** (0.17 g, 0.71 mmol) and CDI (0.23 g, 1.43 mmol); yield: 0.09 g (45%); light-yellow solid, mp: 125–126 °C; $R_f = 0.48$ (EtOAc/MeOH, 95:5); ^{1}H NMR ($CDCl_3$, 500 MHz): $\delta = 5.21$ (s, 2H, CH_2), 6.98 (brs, 1H), 7.00–7.05 (m, 1H), 7.08–7.16 (m, 4H), 7.28–7.31 (m, 2H), 7.64 ppm (brs, 1H, Im-2H); ^{13}C NMR ($CDCl_3$, 125 MHz): $\delta = 44.4$ (CH_2), 116.0, 116.4, 116.6, 117.4, 119.3, 125.1, 123.4, 129.5, 129.8, 137.1, 137.4, 156.5, 154.6, 158.7, 160.2 ppm; HRMS (ESI): calcd for $C_{16}H_{12}F_3N_2$ $[M+H]^+$: 289.0953, found: 289.0955; MS (ESI): $m/z = 289$ $[M+H]^+$.

1-[1-(2,4′-Difluorobiphenyl-4-yl)propyl]-1*H*-imidazole (19). Synthesized according to Method A using **19a** (0.31 g, 1.22 mmol) and CDI (0.40 g, 2.46 mmol); yield: 0.11 g (31%); colorless oil; $R_f = 0.56$ (EtOAc/MeOH, 95:5); ^{1}H NMR ($CDCl_3$, 500 MHz): $\delta = 0.97$ (t, $J = 7.3$ Hz, 3H), 2.21–2.27 (m, 2H), 5.04 (t, $J = 7.7$ Hz, 1H), 6.96–6.99 (m, 2H), 7.02 (dd, $J = 1.9$, 7.9 Hz, 1H), 7.11 (brs, 1H), 7.12 (t, $J = 8.6$ Hz, 2H), 7.37 (t, $J = 7.9$ Hz, 1H), 7.47 (ddd, $J = 1.3$, 5.4, 8.8 Hz, 1H), 7.64 ppm (brs, 1H, Im-2H); ^{13}C NMR ($CDCl_3$, 125 MHz): $\delta = 11.0$ (CH_3), 28.4 (CH_2), 62.5 (CH), 114.3, 115.4, 117.5, 122.4, 127.8, 129.6, 130.5, 131.0, 136.3, 141.8, 141.9, 159.6, 162.5 ppm; HRMS (ESI): calcd for $C_{18}H_{17}F_2N_2$ $[M+H]^+$: 299.1360, found: 299.1351; MS (ESI): $m/z = 299$ $[M+H]^+$.

1-(2,4′-Difluorobiphenyl-4-ylmethyl)-1*H*-imidazole (20). Synthesized according to Method A using **20a** (0.10 g, 0.44 mmol) and CDI (0.40 g, 2.46 mmol); yield: 0.05 g (42%); white solid, mp: 93–94 °C; $R_f = 0.52$ (EtOAc/MeOH, 95:5); ^{1}H NMR ($CDCl_3$, 500 MHz): $\delta = 5.15$ (s, 2H, CH_2), 6.90–6.98 (m, 3H), 7.11–7.13 (m, 2H), 7.25–7.27 (m, 3H), 7.36–7.39 (m, 1H), 7.60 ppm (s, 1H, Im-2H); ^{13}C NMR ($CDCl_3$, 125 MHz) 50.0 (CH_2), 114.9, 115.1, 115.5, 119.3, 123.0, 129.9, 130.6, 130.7, 130.9, 131.2, 137.6, 158.8, 160.8, 161.6, 163.6 ppm; HRMS (ESI): calcd for $C_{16}H_{13}F_2N_2$ $[M+H]^+$: 271.1047, found: 271.1045; MS (ESI): $m/z = 271$ $[M+H]^+$.

1-[1-(2,3′,4′-Trifluorobiphenyl-4-yl)propyl]-1*H*-imidazole (21). Synthesized according to Method A using **21a** (0.28 g, 1.03 mmol) and CDI (0.34 g, 2.06 mmol); yield: 0.09 g (29%); light-brown oil; $R_f = 0.53$ (EtOAc/MeOH, 95:5); ^{1}H NMR ($CDCl_3$, 500 MHz): $\delta = 0.97$ (t, $J = 7.4$ Hz, 3H), 2.20–2.28 (m, 2H), 5.04 (t, $J = 7.6$ Hz, 1H), 6.96–6.99 (m, 2H), 7.03 (dd, $J = 1.9$, 7.9 Hz, 1H), 7.11 (brs, 1H), 7.18–7.23 (m, 2H), 7.31–7.34 (m, 1H), 7.35 (t, $J = 8.0$ Hz, 1H), 7.64 ppm (brs, 1H, Im-2H); ^{13}C NMR ($CDCl_3$, 125 MHz): $\delta = 10.0$ (CH_3), 27.5 (CH_2), 61.5 (CH), 113.5, 116.4, 116.5, 117.0, 121.6, 124.0, 125.8, 128.7, 129.9, 130.8, 135.3, 141.5, 149.0, 149.2, 158.6 ppm; HRMS (ESI): calcd for $C_{18}H_{16}F_3N_2$ $[M+H]^+$: 317.1266, found: 317.1257; MS (ESI): $m/z = 317$ $[M+H]^+$.

1-(2,2′,4′-Trifluorobiphenyl-4-ylmethyl)-1*H*-imidazole (22). Synthesized according to Method A using **22a** (0.10 g, 0.39 mmol) and CDI (0.40 g, 2.46 mmol); yield: 0.06 g (54%); white solid, mp: 112–113 °C; $R_f = 0.47$ (EtOAc/MeOH, 95:5); ^{1}H NMR ($CDCl_3$, 500 MHz): $\delta = 5.21$ (s, 2H, CH_2), 6.90–6.98 (m, 4H), 7.02 (d, $J = 7.8$ Hz, 1H), 7.16 (s, 1H), 7.33–7.35 (m, 2H), 7.85 ppm (s, 1H, Im-2H); ^{13}C NMR ($CDCl_3$, 125 MHz): $\delta = 52.2$ (CH_2), 104.3, 111.5, 114.8, 119.4, 122.8, 129.1, 132.2, 132.2, 137.3, 138.3, 158.9, 161.0, 161.9, 162.0, 164.1 ppm; HRMS (ESI): calcd for $C_{16}H_{12}F_3N_2$ $[M+H]^+$: 289.0953, found: 289.0957; MS (ESI): $m/z = 289$ $[M+H]^+$.

Method B: Grignard reaction. Under exclusion of air and moisture, a solution of EtMgBr (1.0 M, 1.2 equiv) in THF was added dropwise to a solution of the aldehyde or ketone (1 equiv) in THF (12 mL mmol^{-1}). The mixture was stirred overnight at room temperature. Then EtOAc (10 mL) and H_2O (10 mL) were added, and the organic phase was separated. The organic phase was extracted with H_2O and brine, dried over Na_2SO_4, and evaporated under reduced pressure. The crude products were purified by flash chromatography on silica gel.

Method C: Suzuki coupling. The corresponding brominated aromatic compound (1 equiv) was dissolved in toluene (7 mL mmol^{-1}), and an aqueous solution of 2.0 M Na_2CO_3 (3.2 mL mmol^{-1}) and an ethanolic solution (3.2 mL mmol^{-1}) of the corresponding boronic acid (1.5–2.0 equiv) were added. The mixture was deoxygenated under reduced pressure and flushed with N_2. After repeating this cycle several times $Pd(PPh_3)_4$ (4 mol%) was added, and the resulting suspension was heated at reflux for 8 h. After cooling, EtOAc (10 mL) and H_2O (10 mL) were added, and the organic phase was separated. The aqueous phase was extracted with EtOAc (2× 10 mL). The combined organic phases were washed with brine, dried over Na_2SO_4, filtered over a short plug of Celite, and evaporated under reduced pressure. The compounds were purified by flash chromatography on silica gel.

1-(4′-Fluorobiphenyl-4-yl)-1-(1*H*-imidazol-5-yl)-2-methylpropan-1-ol (24). Synthesized according to Method C using 1-(4-bromophenyl)-2-methyl-1-(1-triphenylmethyl-1*H*-imidazol-5-yl)propan-1-ol (0.50 g, 0.93 mmol) and 4-fluorophenylboronic acid (0.23 mg, 1.63 mmol). After workup, the crude was stirred with pyridinium·HCl (0.17 g, 1.5 mmol) in MeOH (40 mL) at 60 °C for 4 h. The

reaction was then quenched by adding saturated $NaHCO_{3(aq)}$ (10 mL). The phases separated after the addition of EtOAc (20 mL). The aqueous phase was extracted with EtOAc (2×20 mL), the combined organic extracts were dried over Na_2SO_4 and concentrated under reduced pressure. The crude product was purified by flash chromatography; yield: 0.21 g (73%); colorless oil; R_f=0.17 (EtOAc/MeOH, 95:5); ^{1}H NMR ($CDCl_3$, 500 MHz): δ=0.82 (d, J=6.8 Hz, 3H), 0.98 (d, J=6.8 Hz, 3H), 2.63–2.65 (m, 1H), 7.01 (s, 1H), 7.10 (dd, J=8.7, 8.8 Hz, 2H), 7.49 (d, J=8.5 Hz, 2H), 7.53 (dd, J=5.4, 8.7 Hz, 2H), 7.58 (s, 1H), 7.62 ppm (d, J=8.3 Hz, 2H); ^{13}C NMR ($CDCl_3$, 125 MHz): δ=17.3, 60.4, 77.7, 115.5, 115.6, 126.2, 126.4, 128.4, 128.5, 133.9, 136.9, 136.9, 138.3, 144.8, 161.4, 163.3 ppm; HRMS (ESI): calcd for $C_{19}H_{20}FN_2O$ $[M+H]^+$: 311.1560, found: 311.1559; MS (ESI): m/z=311 $[M+H]^+$.

Method D: Reduction with $NaBH_4$. $NaBH_4$ (2 equiv) was added to an ice-cooled solution of the corresponding aldehyde or ketone (1 equiv) in MeOH (5 mL mmol^{-1}). The resulting mixture was then heated at reflux for 30 min. After cooling to room temperature, the solvent was distilled off under reduced pressure. H_2O (10 mL) was then added, and the resulting mixture was extracted with EtOAc (3×10 mL). The combined organic phases were washed with brine, dried over $MgSO_4$ and evaporated under reduced pressure. Then the desired product was purified by chromatography on silica gel.

Method E: CDI reaction in THF. CDI (2 equiv) was added to a solution of the corresponding alcohol (1 equiv) in THF (10 mL mmol^{-1}). The solution was then heated at reflux (70 °C) for four days. After cooling to room temperature, the mixture was poured into H_2O and extracted with CH_2Cl_2 (3×25 mL). The combined organic phases were washed with brine, dried over $MgSO_4$ and evaporated under reduced pressure. Then the desired product was purified by chromatography on silica gel.

Imidazole-1-carboxylic acid 1-(3′,4′-difluorobiphenyl-4-yl)propyl ester (3). Synthesized according to Method E using **2a** (0.10 g, 0.42 mmol) and CDI (0.14 g, 0.83 mmol); yield: 0.09 g (37%); white solid, mp: 49–50 °C; R_f=0.29 (CH_2Cl_2/MeOH, 95:5); ^{1}H NMR ($CDCl_3$, 500 MHz): δ=1.01 (t, J=14.8 Hz, 3H, CH_3), 2.01–2.21 (q, J=14.8, 15.5 Hz, 2H, CH_2), 5.88 (t, J=15.5 Hz, 1H, CH), 7.15 (s, 1H), 7.22–7.29 (m, 2H), 7.32–7.34 (m, 1H), 7.36–7.38 (m, 1H), 7.46 (d, J=8.2 Hz, 2H), 7.54 (d, J=8.2 Hz, 2H), 8.35 ppm (s, 1H, Im-2H); ^{13}C NMR ($CDCl_3$, 125 MHz): δ=9.9 (CH_3), 28.9 (CH_2), 82.6 (CH), 115.9, 116.1, 117.5, 117.7, 122.4, 122.9, 123.0, 127.3, 127.4, 129.5, 137.8, 140.2, 149.0, 149.1, 151.2 ppm; HRMS (ESI): calcd for $C_{19}H_{17}F_2N_2O_2$ $[M+H]^+$: 343.1258, found: 343.1250; MS (ESI): m/z=343 $[M+H]^+$.

Imidazole-1-carboxylic acid 1-(2′,4′-difluorobiphenyl-4-yl)propyl ester (5). Synthesized according to Method E using **4a** (0.21 g, 0.85 mmol) and CDI (0.28 g, 1.69 mmol); yield: 0.11 g (43%); white solid, mp: 76–77 °C; R_f=0.29 (CH_2Cl_2/MeOH, 95:5); ^{1}H NMR ($CDCl_3$, 500 MHz): δ=1.01 (t, J=14.8 Hz, 3H, CH_3), 2.03–2.19 (q, J=14.8, 15.5 Hz, 2H, CH_2), 5.87 (t, J=15.5 Hz, 1H, CH), 6.89–7.06 (m, 2H), 7.09–7.11 (m, 1H), 7.36–7.40 (m, 1H), 7.45–7.48 (m, 3H), 7.52 (dd, J=1.6, 1.9 Hz, 2H), 8.24 ppm (s, 1H, Im-2H); ^{13}C NMR ($CDCl_3$, 125 MHz): δ=9.9 (CH_3), 28.9 (CH_2), 82.2 (CH), 104.4, 111.7, 117.2, 124.5, 126.8, 129.3, 130.7, 135.5, 136.9, 137.9, 148.0, 158.5, 1160.7, 161.4, 163.4, 171.2 ppm; HRMS (ESI): calcd for $C_{19}H_{17}F_2N_2O_2$ $[M+H]^+$: 343.1258, found: 343.1247; MS (ESI): m/z=343 $[M+H]^+$.

Imidazole-1-carboxylic acid 1-(2′,5′-difluorobiphenyl-4-yl)propyl ester (8). Synthesized according to Method E using **7a** (0.12 g, 0.46 mmol) and CDI (0.15 g, 0.93 mmol); yield: 0.10 g (69%); white solid, mp: 77–78 °C; R_f=0.29 (CH_2Cl_2/MeOH, 95:5); ^{1}H NMR ($CDCl_3$, 500 MHz): δ=1.01 (t, J=14.8 Hz, 3H, CH_3), 2.02–2.20 (q, J=14.8, 15.5 Hz, 2H, CH_2), 5.88 (t, J=15.5 Hz, 1H, CH), 6.93–7.02 (m, 1H), 7.09–7.15 (m, 3H), 7.46–7.48 (m, 3H), 7.52–7.55 (m, 2H), 8.23 ppm (s, 1H, Im-2H); ^{13}C NMR ($CDCl_3$, 125 MHz): δ=9.9 (CH_3), 28.9 (CH_2), 82.2 (CH), 115.5, 116.7, 117.6, 126.9, 127.4, 129.4, 130.2, 135.3, 136.9, 138.4, 148.0, 154.7, 156.7, 157.8, 159.4 ppm; HRMS (ESI): calcd for $C_{19}H_{17}F_2N_2O_2$ $[M+H]^+$: 343.1258, found: 343.1250; MS (ESI): m/z=343 $[M+H]^+$.

Imidazole-1-carboxylic acid 1-(3,4′-difluorobiphenyl-4-yl)propyl ester (10). Synthesized according to Method E using **7a** (0.19 g, 0.75 mmol) and CDI (0.24 g, 1.50 mmol); yield: 0.10 g (69%); colorless oil; R_f=0.29 (CH_2Cl_2/MeOH, 95:5); ^{1}H NMR ($CDCl_3$, 500 MHz): δ=1.01 (t, J=14.8 Hz, 3H, CH_3), 2.02–2.20 (q, J=14.8, 15.5 Hz, 2H, CH_2), 5.88 (t, J=15.5 Hz, 1H, CH), 6.14 (s, 1H), 7.26–7.28 (m, 2H), 7.19–7.25 (m, 1H), 7.34–7.35 (m, 1H), 7.42–7.48 (m, 2H), 7.50–7.53 (m, 2H), 8.22 ppm (s, 1H, Im-2H); ^{13}C NMR ($CDCl_3$, 125 MHz): δ=9.7 (CH_3), 28.1 (CH_2), 82.2 (CH), 114.3, 114.4, 115.8, 116.0, 117.2, 122.9, 128.1, 128.7, 135.3, 137.0, 159.3, 161.3, 161.9, 163.9, 171.1 ppm; HRMS (ESI): calcd for $C_{19}H_{17}F_2N_2O_2$ $[M+H]^+$: 343.1258, found: 343.1250; MS (ESI): m/z=343 $[M+H]^+$.

Imidazole-1-carboxylic acid 3,4′-difluorobiphenyl-4-ylmethyl ester (12). Synthesized according to Method E using **11a** (0.26 g, 1.20 mmol) and CDI (0.39 g, 2.40 mmol); yield: 0.09 g (28%); white solid, mp: 220–221 °C; R_f=0.29 (CH_2Cl_2/MeOH, 95:5); ^{1}H NMR ($CDCl_3$, 500 MHz): δ=5.33 (s, 2H, CH_2), 7.07 (s, 1H), 7.12–7.15 (t, J=17.4 Hz, 2H), 7.20 (s, 1H), 7.29 (d, J=11.0 Hz, 1H), 7.33–7.35 (m, 2H), 7.49–7.52 (m, 2H), 8.32 ppm(s, 1H, Im-2H); ^{13}C NMR ($CDCl_3$, 125 MHz): δ=45.3 (CH_2), 114.3, 115.9, 116.0, 121.1, 123.3, 126.7, 128.6, 128.7, 130.6, 130.7, 143.5, 143.6, 161.8, 162.0, 164.0 ppm; HRMS (ESI): calcd for $C_{17}H_{13}F_2N_2O_2$ $[M+H]^+$: 315.0945, found: 315.0943; MS (ESI): m/z=315 $[M+H]^+$.

(4′-Fluorobiphenyl-4-yl)(1*H*-imidazol-5-yl)methanol (23). A solution of **23a** (0.10 g, 0.20 mmol) in MeOH (5 mL) was stirred with pyridinium·HCl (35 mg, 0.30 mmol) at 60 °C for 4 h. The reaction was then quenched by adding saturated $NaHCO_{3(aq)}$ (10 mL); EtOAc (20 mL) was added, and the phases separated. The aqueous phase was extracted with EtOAc (3×20 mL), the combined organic extracts were dried over Na_2SO_4, and concentrated under reduced pressure. The crude product was purified by flash chromatography; yield: 0.05 g (91%); colorless oil; R_f=0.19 (EtOAc/MeOH, 95:5); ^{1}H NMR ($CDCl_3$+[D_6]DMSO, 500 MHz): δ=2.99 (s, 1H), 5.84 (s, 1H), 6.87 (s, 2H), 7.02–7.06 (m, 2H), 7.41–7.47 ppm (m, 6H); ^{13}C NMR ($CDCl_3$+[D_6]DMSO, 125 MHz): δ=71.2 (COH), 115.8, 116.0, 116.4, 127.2, 127.9, 129.1, 129.4, 137.1, 138.6, 140.7, 142.3, 150.9, 162.1, 164.1 ppm; HRMS (ESI): calcd for $C_{16}H_{14}FN_2O$ $[M+H]^+$: 269.1090, found: 269.1088; MS (ESI):m/z=269 $[M+H]^+$.

5-[1-(4′-Fluorobiphenyl-4-yl)-2-methylprop-1-enyl]-1*H*-imidazole (25). Compound **24** (0.10 mg, 0.32 mol) was held at reflux in an *i*PrOH solution of HCl (10 mL, 3 N) for 2 h. Afterward, the resulting solution was concentrated under reduced pressure and washed with Et_2O (3×25 mL). No further purification was necessary; yield: 0.07 g (77%); colorless oil; R_f=0.29 (EtOAc/MeOH, 95:5); ^{1}H NMR ($CDCl_3$, 500 MHz): δ=1.80 (s, 3H), 2.05 (s, 3H), 6.98 (s, 1H), 7.12 (dd, J=8.7, 8.8 Hz, 2H), 7.19 (d, J=8.3 Hz, 2H), 7.50 (d, J=8.3 Hz, 2H), 7.54 (dd, J=5.3, 8.7 Hz, 2H), 7.63 ppm (s, 1H); ^{13}C NMR ($CDCl_3$, 125 MHz): δ=22.7 (CH_3), 23.1 (CH_3), 115.6, 115.8, 123.4, 125.2, 126.9, 128.5, 128.5, 129.8, 130.3, 132.6, 133.6, 133.7, 134.9, 136.6, 136.7, 136.7, 137.1, 138.8, 139.8, 160.9, 161.5 ppm; ^{19}F NMR ($CDCl_3$, 400 MHz): δ=−115.56 ppm (s, 1F); HRMS (ESI): calcd for $C_{19}H_{18}FN_2$ $[M+H]^+$: 293.1454, found: 293.1455; MS (ESI):m/z=293 $[M+H]^+$.

5-[1-(4′-Fluorobiphenyl-4-yl)-2-methylpropyl]-1*H*-imidazole (26). Pearlman's catalyst (5 mg, 7.12 μmol) and **25** (50 mg, 0.17 mmol) were prepared in EtOH and THF (2:1, 5 mL) under H_2 atmosphere.

The mixture was left stirring for 3 h, then the catalyst was filtered off three times, and the solution was concentrated under reduced pressure. The obtained solid was washed with Et_2O (3×25 mL). No further purification was necessary; yield: 50 mg (100%); yield: 0.07 g (77%); colorless oil; R_f=0.29 (EtOAc/MeOH, 95:5); ^{1}H NMR ($CDCl_3$, 500 MHz): δ=0.86 (d, J=6.6 Hz, 3H, CH_3), 0.99 (d, J=6.6 Hz, 3H, CH_3), 3.60 (d, J=9.4 Hz, 1H, CH), 6.90 (s, 1H), 7.09 (dd, J=8.7, 8.8 Hz, 2H), 7.36 (d, J=8.2 Hz, 2H), 7.45 (d, J=8.2 Hz, 2H), 7.51 (dd, J=5.4, 8.7 Hz, 2H), 7.55 ppm (s, 1H); ^{13}C NMR ($CDCl_3$, 125 MHz): δ=21.2, 21.8, 32.5, 51.9, 115.4, 115.6, 123.1, 126.9, 128.4, 128.5, 128.9, 134.4, 137.1, 138.1, 142.4 ppm; HRMS (ESI): calcd for $C_{19}H_{20}FN_2$ $[M+H]^+$: 295.1611, found: 295.1605; MS (ESI):m/z=295 $[M+H]^+$.

Docking studies

Ligands: All molecular modeling studies were performed on an Intel P4 CPU 3.00 GHz running Linux CentOS5.2. The structures of the inhibitors were built with SYBYL 8 (Sybyl, Tripos Inc., St. Louis, MO, USA) and energy minimized in the MMFF94s force field[25] as implemented in SYBYL.

Docking: Molecular docking calculations were performed for various inhibitors listed in Table 1. Because the GOLD docking program allows flexible docking of the compounds, no conformational search was employed to the ligand structures. GOLD gave the best poses by a genetic algorithm (GA) search strategy. Ligands were docked in 50 independent genetic algorithm runs for each of the three GOLD docking runs. Heme iron was chosen as the active site origin, while the radius was at 19 Å. The automatic active site detection was switched on. A distance constraint of a minimum of 1.9 and a maximum of 2.5 Å between the sp^2-hybridised nitrogen of the imidazole and the iron was set. Additionally, the goldscore.p450_pdb parameters were used, and some of the GoldScore parameters were modified to improve the weight of hydrophobic interaction and of the coordination between iron and nitrogen. The genetic algorithm default parameters were set as suggested by the GOLD authors. On the other hand, the annealing parameters of fitness function were set at 3.5 Å for hydrogen bonding and 6.5 Å for van der Waals interactions.

Analogously as for GOLD, no conformational search was performed prior docking with FlexX, as the ligands are docked according to an incremental fragment docking strategy. Standard parameter settings were used except for "base placement", which was set on single interaction scan, and "chemical parameters", in which the maximum overlap volume of the subroutine "clash handling" was set at a range of 3.6 Å. Additionally the "FlexX-Pharm" module was employed, setting the heme iron as an octahedral coordinating metal pharmacophore point. The very same iron atom was chosen as active site center, and amino acid residues within 16 Å were considered as part of the active site.

All the poses resulting from three docking runs (GOLD–ChemScore, GOLD–GoldScore, and FlexX) for each compound were clustered with ACIAP,[19] and the representative structure of each significant cluster was selected. After the docking simulations and cluster analysis were performed, the quality of the docked representative poses was evaluated based on visual inspection of the putative binding modes of the ligands. The latter were further evaluated by MOE (http://www.chemcmpd.com) with its LigX module and evaluated by means of the various scoring functions (GoldScore, ChemScore, and the empirical FlexX Score).

MEP: For each docked compound, geometry optimization was performed by using the B3LYP hybrid functional[20] in combination with a 6-311++G (d,p) basis set using the Gaussian 03 software package.[21] The molecular electrostatic potential (MEP) maps were plotted using GaussView 3.0, the 3D molecular graphics package of Gaussian. These electrostatic potential surfaces were generated by mapping 6-311++G** electrostatic potentials onto surfaces of molecular electron density (isovalue=0.004 electron Å^{-1}) and the ESP values on the surface are color coded, ranging from -6 kcal mol^{-1} (red) to $+12$ kcal mol^{-1} (blue).

Acknowledgements

The authors thank Dr. Ursula Müller-Vieira and Maria-Christina Scherzberg for IC_{50} determinations, Dr. Klaus Biemel for performing the in vivo tests, and Dr. Kerstin Jahn-Hoffmann, Dr. Mariano E. Pinto-Bazurco Mendieta and Dr. Marc Bartels for help in the synthesis of some compounds. The authors also appreciate the kind help from Prof. Dr. Rolf Müller (Saarland University, Saarbrücken, Germany) in performing HRMS.

Keywords: anticancer agents · cytochrome P450 inhibitors · fluorine · pharmacokinetics · prostate cancer

[1] A. Jemal, R. Siegel, E. Ward, Y. Hao, J. Xu, T. Murray, M. J. Thun, *CA Cancer J. Clin.* **2008**, *58*, 71–96.

[2] I. Huhtaniemi, H. Nikula, M. Parvinen, S. Rannikko, *Am. J. Clin. Oncol.* **1988**, *11* (Suppl. 1), S11–S15.

[3] F. Labrie, A. Dupont, A. Belanger, L. Cusan, Y. Lacourciere, G. Monfette, J. G. Laberge, J. P. Emond, A. T. Fazekas, J. P. Raynaud, J. M. Husson, *Clin. Invest. Med.* **1982**, *5*, 267–275.

[4] a) T. Hara, J. Miyazaki, H. Araki, M. Yamaoka, N. Kanzaki, M. Kusaka, M. Miyamoto, *Cancer Res.* **2003**, *63*, 149–153; b) X. Y. Zhao, P. J. Malloy, A. V. Krishnan, S. Swami, N. M. Navone, D. M. Peehl, D. Feldman, *Nat. Med.* **2000**, *6*, 703–706.

[5] a) C. I. Herold, K. L. Blackwell, *Clin. Breast Cancer* **2008**, *8*, 50–64; b) R. W. Hartmann, H. Bayer, G. Grün, *J. Med. Chem.* **1994**, *37*, 1275–1281; c) F. Leonetti, A. Favia, A. Rao, R. Aliano, A. Paluszcak, R. W. Hartmann, A. Carotti, *J. Med. Chem.* **2004**, *47*, 6792–6803; d) M. Le Borgne, P. Marchand, M. Duflos, B. Delevoye-Seiller, S. Piessard-Robert, G. Le Baut, R. W. Hartmann, M. Palzer, *Arch. Pharm.* **1997**, *330*, 141–145; e) M. P. Lézé, M. Le Borgne, P. Pinson, A. Palusczak, M. Duflos, G. Le Baut, R. W. Hartmann, *Bioorg. Med. Chem. Lett.* **2006**, *16*, 1134–1137; f) S. Gobbi, A. Cavalli, A. Rampa, F. Belluti, L. Piazzi, A. Paluszcak, R. W. Hartmann, M. Recanatini, A. Bisi, *J. Med. Chem.* **2006**, *49*, 4777–4780; g) A. Cavalli, A. Bisi, C. Bertucci, C. Rosini, A. Paluszcak, S. Gobbi, E. Giorgio, A. Rampa, F. Belluti, L. Piazzi, P. Valenti, R. W. Hartmann, M. Recanatini, *J. Med. Chem.* **2005**, *48*, 7282–7289; h) S. Castellano, G. Stefancich, R. Ragno, K. Schewe, M. Santoriello, A. Caroli, R. W. Hartmann, G. Sbardella, *Bioorg. Med. Chem.* **2008**, *16*, 8349–8358.

[6] a) S. Lucas, R. Heim, C. Ries, K. E. Schewe, B. Birk, R. W. Hartmann, *J. Med. Chem.* **2008**, *51*, 8077–8087; b) S. Lucas, R. Heim, M. Negri, I. Antes, C. Ries, K. E. Schewe, A. Bisi, S. Gobbi, R. W. Hartmann, *J. Med. Chem.* **2008**, *51*, 6138–6149; c) R. Heim, S. Lucas, C. M. Grombein, C. Ries, K. E. Schewe, M. Negri, U. Müller-Vieira, B. Birk, R. W. Hartmann, *J. Med. Chem.* **2008**, *51*, 5064–5074; d) M. Voets, I. Antes, C. Scherer, U. Müller-Vieira, K. Biemel, S. Marchais-Oberwinkler, R. W. Hartmann, *J. Med. Chem.* **2006**, *49*, 2222–2231; e) M. Voets, I. Antes, C. Scherer, U. Müller-Vieira, K. Biemel, C. Barassin, S. Marchais-Oberwinkler, R. W. Hartmann, *J. Med. Chem.* **2005**, *48*, 6632–6642; f) S. Ulmschneider, U. Müller-Vieira, C. D. Klein, I. Antes, T. Lengauer, R. W. Hartmann, *J. Med. Chem.* **2005**, *48*, 1563–1575; g) S. Ulmschneider, U. Müller-Vieira, M. Mitrenga, R. W. Hartmann, S. Oberwinkler-Marchais, C. D. Klein, M. Bureik, R. Bernhardt, I. Antes, T. Lengauer, *J. Med. Chem.* **2005**, *48*, 1796–1805.

[7] B. C. Chung, J. Picardo-Leonard, M. Hanui, M. Bienkowski, P. F. Hall, J. E. Shively, W. L. Miller, *Proc. Natl. Acad. Sci. USA* **1987**, *84*, 407 – 411.
[8] a) K. A. Harris, V. Weinberg, R. A. Bok, M. Kakefuda, E. J. Small, *J. Urol.* **2002**, *168*, 542 – 545; b) J. Eklund, M. Kozloff, J. Vlamakis, A. Starr, M. Mariott, L. Gallot, B. Jovanovic, L. Schilder, E. Robin, M. Pins, R. C. Bergan, *Cancer* **2006**, *106*, 2459 – 2465.
[9] a) G. A. Potter, S. E. Banie, M. Jarman, M. G. Rowlands, *J. Med. Chem.* **1995**, *38*, 2463 – 2471; b) J. P. Burkhart, C. A. Gates, M. E. Laughlin, R. J. Resvick, N. P. Peet, *Bioorg. Med. Chem.* **1996**, *4*, 1411 – 1420; c) V. D. Handratta, T. S. Vasaitis, V. C. O. Njar, L. K. Gediya, R. Kataria, P. Chopra, D. Newman, Jr., R. Farquhar, Z. Guo, Y. Qiu, A. M. H. Brodie, *J. Med. Chem.* **2005**, *48*, 2972 – 2984; d) V. C. O. Njar, K. Kato, I. P. Nnane, D. N. Grigoryev, B. J. Long, A. M. H. Brodie, *J. Med. Chem.* **1998**, *41*, 902 – 912.
[10] a) R. W. Hartmann, M. Hector, M. Haidar, P. B. Ehmer, W. Reichert, J. Jose, *J. Med. Chem.* **2000**, *43*, 4266 – 4277; b) R. W. Hartmann, M. Hector, B. G. Wachall, A. Palusczak, M. Palzer, V. Huch, M. Veith, *J. Med. Chem.* **2000**, *43*, 4437 – 4445; c) V. C. O. Njar, M. Hector, R. W. Hartmann, *Bioorg. Med. Chem.* **1996**, *4*, 1447 – 1453; d) S. Haidar, P. B. Ehmer, R. W. Hartmann, *Arch. Pharm.* **2001**, *334*, 373 – 374.
[11] a) G. A. Wächter, R. W. Hartmann, T. Sergejew, G. L. Grün, D. Ledergerber, *J. Med. Chem.* **1996**, *39*, 834 – 841; b) F. C. Y. Chan, G. A. Potter, S. E. Barrie, B. P. Haynes, M. G. Rowlands, G. Houghton, M. Jarman, *J. Med. Chem.* **1996**, *39*, 3319 – 3323.
[12] a) B. G. Wachall, M. Hector, Y. Zhuang, R. W. Hartmann, *Bioorg. Med. Chem.* **1999**, *7*, 1913 – 1924; b) Y. Zhuang, B. G. Wachall, R. W. Hartmann, *Bioorg. Med. Chem.* **2000**, *8*, 1245 – 1252; c) F. Leroux, T. U. Hutschenreuter, C. Charriere, R. Scopelliti, R. W. Hartmann, *Helv. Chim. Acta* **2003**, *86*, 2671 – 2686; d) T. U. Hutschenreuter, P. E. Ehmer, R. W. Hartmann, *J. Enzyme Inhib. Med. Chem.* **2004**, *19*, 17 – 32; e) C. Jagusch, M. Negri, U. E. Hille, Q. Hu, M. Bartels, K. Jahn-Hoffmann, M. A. E. Pinto-Bazurco Mendieta, B. Rodenwaldt, U. Müller-Vieira, D. Schmidt, T. Lauterbach, M. Recanatini, A. Cavalli, R. W. Hartmann, *Bioorg. Med. Chem.* **2008**, *16*, 1992 – 2010; f) M. A. E. Pinto-Bazurco Mendieta, M. Negri, C. Jagusch, U. E. Hille, U. Müller-Vieira, D. Schmidt, K. Hansen, R. W. Hartmann, *Bioorg. Med. Chem. Lett.* **2008**, *18*, 267 – 273; g) Q. Hu, M. Negri, K. Jahn-Hoffmann, Y. Zhuang, S. Olgen, M. Bartels, U. Müller-Vieira, T. Lauterbach, R. W. Hartmann, *Bioorg. Med. Chem.* **2008**, *16*, 7715 – 7727; h) M. A. E. Pinto-Bazurco Mendieta, M. Negri, C. Jagusch, U. Müller-Vieira, T. Lauterbach, R. W. Hartmann, *J. Med. Chem.* **2008**, *51*, 5009 – 5018; i) U. E. Hille, Q. Hu, C. Vock, M. Negri, M. Bartels, U. Müller-Vieira, T. Lauterbach, R. W. Hartmann, *Eur. J. Med. Chem.* **2009**, *44*, 2765 – 2775; j) M. A. E. Pinto-Bazurco Mendieta, M. Negri, Q. Hu, U. E. Hille, C. Jagusch, K. Jahn-Hoffmann, U. Müller-Vieira, D. Schmidt, T. Lauterbach, R. W. Hartmann, *Arch. Pharm.* **2008**, *341*, 597 – 609; k) U. E. Hille, Q. Hu, M. A. E. Pinto-Bazurco Mendieta, M. Bartels, C. A. Vock, T. Lauterbach, R. W. Hartmann, *Comptes Rendus Chim.* **2009**, *12*, 1117 – 1126.
[13] a) W. K. Hagmann, *J. Med. Chem.* **2008**, *51*, 4359 – 4369; b) H. J. Böhm, D. Banner, S. Bendels, M. Kansy, B. Kuhn, K. Müller, U. Obst-Sander, M. Stahl, *ChemBioChem* **2004**, *5*, 637 – 643; c) K. Müller, C. Faeh, F. Diederich, *Science* **2007**, *317*, 1881 – 1886; d) S. DiMagno, H. Sun, *Curr. Top. Med. Chem.* **2006**, *6*, 1473 – 1482; e) R. Paulini, K. Müller, F. Diederich, *Angew. Chem.* **2005**, *117*, 1820 – 1839; *Angew. Chem. Int. Ed.* **2005**, *44*, 1788 – 1805; f) J. A. Olsen, D. W. Banner, P. Seiler, U. O. Sander, A. D'Arcy, M. Stihle, K. Müller, F. Diederich, *Angew. Chem.* **2003**, *115*, 2611 – 2615; *Angew. Chem. Int. Ed.* **2003**, *42*, 2507 – 2511; g) J. A. Olsen, D. W. Banner, P. Seiler, B. Wagner, T. Tschopp, U. Obst-Sander, M. Kansy, K. Müller, F. Diederich, *ChemBioChem* **2004**, *5*, 666 – 675; h) F. Hof, D. M. Scofield, W. B. Schweizer, F. Diederich, *Angew. Chem.* **2004**, *116*, 5166 – 5169; *Angew. Chem. Int. Ed.* **2004**, *43*, 5056 – 5059; i) E. S. Istvan, J. Deisenhofer, *Science* **2001**, *292*, 1160 – 1164; j) G. Phillips, D. D. Davey, K. A. Eagen, S. K. Koovakkat, A. Liang, H. P. Ng, M. Pinkerton, L. Trinh, M. Whitlow, A. M. Beatty, M. M. Morrissey, *J. Med. Chem.* **1999**, *42*, 1749 – 1756; k) J. J. Parlow, A. M. Stevens, R. A. Stegeman, W. C. Stallings, R. G. Kurumbail, M. S. South, *J. Med. Chem.* **2003**, *46*, 4297 – 4312; l) J. J. Parlow, R. G. Kurumbail, R. A. Stegeman, A. M. Stevens, W. C. Stallings, M. S. South, *J. Med. Chem.* **2003**, *46*, 4696 – 4701; m) B. K. Park, N. R. Kitteringham, P. M. O'Neill, *Annu. Rev. Pharmacol. Toxicol.* 2001, 41, 443 – 470.
[14] N. Miyaura, A. Suzuki, *Chem. Rev.* **1995**, *95*, 2457 – 2483.
[15] Y. Tang, Y. Dong, J. L. Vennerstrom, *Synthesis* **2004**, *15*, 2540 – 2544.
[16] P. B. Ehmer, J. Jose, R. W. Hartmann, *J. Steroid Biochem. Mol. Biol.* **2000**, *75*, 57 – 63.
[17] a) G. Jones, P. Willett, R. C. Glen, A. R. Leach, R. Taylor, *J. Mol. Biol.* **1997**, *267*, 727 – 748; b) M. L. Verdonk, J. C. Cole, M. J. Hartshorn, C. W. Murray, R. D. Taylor, *Proteins* **2003**, *52*, 609 – 623.
[18] a) B. Kramer, M. Rarey, T. Lengauer, *Proteins Struct. Funct. Genet.* **1999**, *37*, 228 – 241; b) FlexX trial version 3.1.3, BioSolveIT GmbH, Sankt Augustin (Germany), http://www.biosolveit.de/ (accessed March 7, 2010).
[19] a) G. Bottegoni, A. Cavalli, M. A. Recanatini, *J. Chem. Inf. Model.* **2006**, *46*, 852 – 862; b) G. Bottegoni, W. Rocchia, M. Recanatini, A. Cavalli, *Bioinformatics* **2006**, *22*, e58 – e65.
[20] a) A. D. Becke, *J. Chem. Phys.* **1993**, *98*, 5648 – 5652; b) P. J. Stephens, F. J. Devlin, C. F. Chabalowski, M. J. Frisch, *J. Phys. Chem.* **1994**, *98*, 11623 – 11627.
[21] Gaussian 03, Revision C.02: M. J. Frisch, G. W. Trucks, H. B. Schlegel, G. E. Scuseria, M. A. Robb, J. R. Cheeseman, J. A. Montgomery, Jr., T. Vreven, K. N. Kudin, J. C. Burant, J. M. Millam, S. S. Iyengar, J. Tomasi, V. Barone, B. Mennucci, M. Cossi, G. Scalmani, N. Rega, G. A. Petersson, H. Nakatsuji, M. Hada, M. Ehara, K. Toyota, R. Fukuda, J. Hasegawa, M. Ishida, T. Nakajima, Y. Honda, O. Kitao, H. Nakai, M. Klene, X. Li, J. E. Knox, H. P. Hratchian, J. B. Cross, V. Bakken, C. Adamo, J. Jaramillo, R. Gomperts, R. E. Stratmann, O. Yazyev, A. J. Austin, R. Cammi, C. Pomelli, J. W. Ochterski, P. Y. Ayala, K. Morokuma, G. A. Voth, P. Salvador, J. J. Dannenberg, V. G. Zakrzewski, S. Dapprich, A. D. Daniels, M. C. Strain, O. Farkas, D. K. Malick, A. D. Rabuck, K. Raghavachari, J. B. Foresman, J. V. Ortiz, Q. Cui, A. G. Baboul, S. Clifford, J. Cioslowski, B. B. Stefanov, G. Liu, A. Liashenko, P. Piskorz, I. Komaromi, R. L. Martin, D. J. Fox, T. Keith, M. A. Al-Laham, C. Y. Peng, A. Nanayakkara, M. Challacombe, P. M. W. Gill, B. Johnson, W. Chen, M. W. Wong, C. Gonzalez, J. A. Pople, Gaussian Inc., Wallingford, CT (USA), **2004**.
[22] GaussView 3.0: I. Dennington, K. T. Roy, J. Millam, K. Eppinnett, W. L. Howell, R. Gilliland, Semichem Inc., Shawnee Mission, KS (USA), **2003**.
[23] a) E. Bey, S. Marchais-Oberwinkler, M. Negri, P. Kruchten, A. Oster, T. Klein, A. Spadaro, R. Werth, M. Frotscher, B. Birk, R. W. Hartmann, *J. Med. Chem.* **2009**, *52*, 6724 – 6743; b) P. Kruchten, R. Werth, E. Bey, A. Oster, S. Marchais-Oberwinkler, M. Frotscher, R. W. Hartmann, *J. Steroid Biochem. Mol. Biol.* **2009**, *114*, 200 – 206; c) E. Bey, S. Marchais-Oberwinkler, R. Werth, M. Negri, Y. A. Al-Soud, P. Kruchten, A. Oster, M. Frotscher, B. Birk, R. W. Hartmann, *J. Med. Chem.* **2008**, *51*, 6725 – 6739; d) S. Marchais-Oberwinkler, P. Kruchten, M. Frotscher, E. Ziegler, A. Neugebauer, U. Bhoga, E. Bey, U. Müller-Vieira, J. Messinger, H. Thole, R. W. Hartmann, *J. Med. Chem.* **2008**, *51*, 4685 – 4698; e) M. Frotscher, E. Ziegler, S. Marchais-Oberwinkler, P. Kruchten, A. Neugebauer, L. Fetzer, C. Scherer, U. Müller-Vieira, J. Messinger, H. Thole, R. W. Hartmann, *J. Med. Chem.* **2008**, *51*, 2158 – 2169.
[24] a) F. Picard, T. Schulz, R. W. Hartmann, *Bioorg. Med. Chem.* **2002**, *10*, 437 – 448; b) E. Baston, A. Palusczak, R. W. Hartmann, *Eur. J. Med. Chem.* **2000**, *35*, 931 – 940; c) W. Reichert, J. Jose, R. W. Hartmann, *Arch. Pharm.* **2000**, *333*, 201 – 204; d) F. Picard, E. Baston, W. Reichert, R. W. Hartmann, *Bioorg. Med. Chem.* **2000**, *8*, 1479 – 1487; e) E. Baston, R. W. Hartmann, *Bioorg. Med. Chem. Lett.* **1999**, *9*, 1601 – 1606.
[25] T. A. Halgren, *J. Comput. Chem.* **1999**, *20*, 730 – 748.

Received: February 15, 2010
Revised: March 22, 2010
Published online on April 30, 2010

